ENCLOSURE 2

MFN 06-011

NEDO-33083, Supplement 2, "TRACG Application for

ESBWR Anticipated Transient Without Scram Analyses,"

December 2005

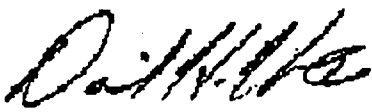General Electric Company

Licensing Topical Report

TRACG Application
for
ESBWR Anticipated Transient Without Scram Analyses

W. Marquino
S. Sitaraman
B. Shiralkar

Approved:

D. Hinds, ESBWR Engineering Manager

IMPORTANT NOTICE REGARDING CONTENTS OF THIS REPORT
PLEASE READ CAREFULLY

ACKNOWLEDGMENTS

ACRONYMS AND ABBREVIATIONS

ABWR	Advanced Boiling Water Reactor
AL	Analytical Limit
AOO	Anticipated Operational Occurrence
ARI	Alternate Rod Insertion
ASME	American Society of Mechanical Engineers
ATWS	Anticipated Transients Without Scram
BOC	Beginning of Cycle
BWR	Boiling Water Reactor
BWR/n	GE BWR product line n (n can be 2, 3, 4, 5, or 6)
CSAU	Code Scaling, Applicability, and Uncertainty
CTR	Customer Technical Requirement
dP	Differential Pressure
ESBWR	Economic Simplified Boiling Water Reactor
EOC	End of Cycle
EOP	Emergency Operating Procedures
FMCRD	Fine Motion Control Rod Drive
FW	Feedwater
GE	General Electric Company
GE13	GE fuel product line 13
GE14	GE fuel product line 14
GESTAR	GE Standard Application for Reactor Fuel
LCV	Loss of Condenser Vacuum ATWS Event
LFWH	Loss of Feedwater Heating ATWS Event
LOCA	Loss of Coolant Accident
LTR	Licensing Topical Report
MCNP	Monte Carlo Neutral Particle Transport Code
MELLLA+	Maximum Extended Load Line Limit Analysis Plus
MOC	Middle of Cycle
MSIV	Main Steam Isolation Valve
MSIVC	MSIV Closure ATWS Event
MSIVF	MSIV Closure with Flux Scram AOO

MWth	Mega-Watt Thermal
NRC	United States Nuclear Regulatory Commission
ODYN	One-Dimensional Reactor Dynamics Code
OSUTL	One Sided Upper Tolerance Limit
$OSUTL_{x/y}$	One Side Upper Tolerance Limit with x% content at y% confidence
PANACEA	Three-Dimensional BWR Core Steady State Simulator Code
PCT	Peak Clad Temperature
PIRT	Phenomena Importance and Ranking Table
PRFO	Pressure Regulator Failed Open ATWS Event
RCPB	Reactor Coolant Pressure Boundary
RHR	Residual Heat Removal
rms	Root Mean Square
RPS	Reactor Protection System
RPT	Recirculation Pump Trip
RPV	Reactor Pressure Vessel
RWCU/SDC	Reactor Water Cleanup/Shutdown Cooling System
S/RV	Safety/Relief Valve
SBWR	Simplified Boiling Water Reactor
SCRRI	Select Control Rod Run-In
SER	Safety Evaluation Report
SLCS	Standby Liquid Control System
SRP	Standard Review Plan
SRV	Safety Relief Valve
TASC	Single Channel Transient Analysis Code
TCV	Turbine Control Valve
TGBLA	Lattice Physics Design Code
TRACG	GE version of the Transient Reactor Analysis Code

CONTENTS

LIST OF FIGURES

LIST OF TABLES

ABSTRACT

This report discusses the application of TRACG, the General Electric (GE) proprietary version of the Transient Reactor Analysis Code, to analyses of Anticipated Transient Without Scram (ATWS) for Economic Simplified Boiling Water Reactors (ESBWRs). Realistic calculations with TRACG can be used to support licensing evaluations for these transient events. The information presented in this report is an extension to the information submitted for TRACG Application to ESBWR Stability, Anticipated Operational Occurrences (AOOs), LOCA ECCS and Containment analysis.

1.0 INTRODUCTION

1.1 Background

Anticipated operational occurrences are those conditions of normal operation that are expected to occur one or more times during the life of the nuclear power unit. An Anticipated Transient Without Scram (ATWS) is an Anticipated Operational Occurrence (AOO), followed by the failure of the reactor trip portion of the protection system.

GE ATWS analysis of jet pump BWRs has been performed with ODYN in accordance with Reference 5. The ODYN code along with the TASC code [9] is used to determine peak vessel pressure and Peak Clad Temperature (PCT) [3]. For the suppression pool heat-up, the method includes an energy balance on the suppression pool, considering the Safety/Relief Valve (S/RV) steam flow, Residual Heat Removal (RHR) heat exchanger capacity, initial suppression pool conditions, and service water temperature. The NRC approved the use of TRACG for calculation of ATWS peak vessel pressure in accordance with Reference 8

Reference 1 provides the licensing basis for the TRACG application to ESBWR LOCA ECCS and Containment Analysis. The U. S. Nuclear Regulatory Commission (NRC) Safety Evaluation Report (SER) for Reference 1 explicitly excluded ATWS and stability from the scope of evaluation.

This report describes an application methodology for ATWS analysis of ESBWR vessel pressure, clad temperature and suppression pool temperature using TRACG consistent with References 1, 8 and 12. As much as possible, this reports references or follows analysis models, nodalization, procedures, tests and qualification, which have previously been submitted or approved by the NRC.

Some areas of ATWS analysis involve phenomena or models that have not been reviewed in the NRC's review of prior TRACG applications. Justification is provided that TRACG can model these phenomena or that the application methodology bounds the phenomenon, and that the models are qualified by comparisons to tests or alternate methods.

1.2 Summary

This document demonstrates the acceptable use of TRACG analysis results for licensing ESBWR power plants within the applicable licensing bases. GE has provided information to support the use of TRACG as a method of analyzing ESBWR ATWS to provide reasonable assurance that applicable licensing limits are not exceeded.

[[Proprietary Information Redacted]]

1.3 Scope of Review

GE requests that the NRC approve TRACG for use in analysis of ESBWR ATWS transients.

2.0 LICENSING REQUIREMENTS AND SCOPE OF APPLICATION

2.1   10CFR50 Appendix A

Anticipated Transient Without Scram (ATWS) means an Anticipated Operational Occurrence (AOO) as defined in Appendix A, followed by the failure of the reactor trip portion of the protection system specified in General Design Criterion 20 of Appendix A of 10CFR50.

2.2   10CFR50.62

This section specifies the features required in a BWR to mitigate ATWS. It requires the BWR to have:

1) An ARI system that utilizes sensors and logic which are diverse and independent of the RPS,

2) An automatic standby liquid control system (SLCS) with a minimum capacity equivalent to 5.42E-3 m3/sec (86 gpm) of 13 weight percent sodium pentaborate solution.

3) Automatic recirculation pump trip (RPT)

Information must be provided to the NRC to demonstrate that these items are adequate.

ATWS prevention/mitigation features of ESBWR include:

1) An ARI system that utilizes sensors and logic which are diverse and independent of the RPS,

2) An automatic standby liquid control system (SLCS) with a minimum capacity equivalent to 5.42E-3 m3/sec (86 gpm) of 13 weight percent sodium pentaborate solution,

3) Electrical insertion of FMCRDs that also utilize sensors and logic which are diverse and independent of the RPS, and

4) Automatic feedwater runback under conditions indicative of an ATWS.

10CFR50.62 prescribes hardware requirements, rather than acceptance criteria. BWR performance with the required hardware had been shown to meet specific acceptance criteria in Reference 3. Since the ESBWR uses natural circulation, there are no recirculation pumps to be tripped. Hence, no RPT logic is implemented in the ESBWR. Two additional mitigation features are provided, electrical insertion of control rods, which is diverse from the hydraulic scram and ARI, and an ATWS automatic feedwater runback feature.

The purpose of ESBWR ATWS analysis is to demonstrate that the ESBWR mitigation features are adequate with respect to the same criteria used to evaluate the 10CFR50.46 hardware requirements for forced recirculation plants in Reference 3. Those criteria are:

Fuel Integrity - The long term core cooling capacity is assured by meeting the cladding temperature and oxidation criteria of 10CFR50.46 (i.e. peak cladding temperature not exceeding 1200°C (2200°F), and the local oxidation of the cladding not exceeding 17% of the total cladding thickness).

Primary System − Reactor Pressure Vessel integrity is assured by limiting the maximum primary stress within the reactor coolant pressure boundary (RCPB) to the emergency limits as defined in the ASME Code, Section III.

Containment Integrity - The long term containment capability is assured by limiting the maximum containment pressure to the design pressure of the containment structure and the suppression pool temperature to the wetwell design temperature.

Long-Term Shutdown Cooling - Subsequent to an ATWS event, the reactor shall be brought to a safe shutdown condition, and be cooled down and maintained in a cold shutdown condition.

2.3 Standard Review Plan Guidelines (NUREG 800)

The guidelines provided in the Standard Review Plan 15.8, ATWS [2] predate 10CFR50.62.

2.4 Current Implementation and Practices

The licensing basis analysis of AOOs must be performed with an approved model and analysis assumptions. The ODYN code [5] has been accepted by the NRC for use in ATWS analysis. TRACG has model capabilities that exceed those in ODYN and has been qualified against a wider range of data.

NRC Staff Report for ATWS events is described in NUREG–0460 [10].

[[Proprietary Information Redacted]]

2.5 Proposed Application Methodology

2.5.1 Conformance with CSAU Methodology

The proposed application methodology using TRACG for ATWS transient analyses considers the elements of the NRC-developed CSAU evaluation methodology [6]. The CSAU report describes a rigorous process for evaluating the total model and plant parameter uncertainty for a nuclear power plant calculation. The rigorous process for applying realistic codes and quantifying the overall model and plant parameter uncertainties appears to represent the best available practice. While the CSAU methodology was developed for application to Loss-Of-Coolant Accidents (LOCAs), there are no technical reasons that prevent CSAU methodology from being applied to other event scenarios such as ATWS.

[[Proprietary Information Redacted]]

2.5.2 Advantages of TRACG Compared to the Current Process

The primary advantage of TRACG over the current process used for ATWS transient analyses is:

- [[Proprietary Information Redacted]]

2.6 Implementation Requirements

The implementation of TRACG into actual licensing analysis is contingent on completion of the following implementation requirements:

- Review and approval by the NRC of the process for analyzing ATWS events described in Section 6, 7 and 8.

2.7 Review Requirements For Updates

In order to effectively manage the future viability of TRACG for ATWS licensing calculations, GE proposes the following requirements for upgrades to the code to define changes that (1) require NRC review and approval and (2) that will be on a notification basis only.

2.7.1 Updates to TRACG Code

Modifications to the basic models described in Reference 14 may <u>not</u> be used for ATWS licensing calculations without NRC review and approval.

Updates to the TRACG nuclear methods to ensure compatibility with the NRC-approved steady-state nuclear methods (e.g., PANAC11) may be used for ATWS licensing calculations without NRC review and approval as long as the peak vessel pressure, fuel temperature and suppression pool temperature shows less than 1 sigma deviation difference compared to the method presented in this LTR. A typical ATWS in each of the event scenarios will be compared and the results from the comparison will be transmitted for information.

Changes in the numerical methods to improve code convergence may be used in ATWS licensing calculations without NRC review and approval.

Features that support effective code input/output may be added without NRC review and approval.

2.7.2 Updates to TRACG Model Uncertainties

New data may become available with which the specific model uncertainties described in Section 5.0 may be reassessed. If the reassessment results in a need to change specific model uncertainty, the specific model uncertainty may be revised for ATWS licensing calculations without NRC review and approval as long as the process for determining the uncertainty is unchanged.

The nuclear uncertainties (void coefficient and Doppler coefficient) may be revised without review and approval as long as the process for determining the uncertainty is unchanged. The revised uncertainties will be used to confirm the conservatism of the calculation. In all cases, changes made to model uncertainties done without review and approval will be transmitted for information.

2.7.3 Updates to TRACG Application Method

Revisions to the TRACG application method described in Section 7 may not be used for ATWS licensing calculations without NRC review and approval.

2.8 ATWS Scenario Specification

The events that must be considered for ATWS analysis are the Anticipated Operational Occurrences (AOOs). AOO transient events include:

1. Pressurization events, including: turbine trip, load rejection, main steam line isolation valve closure.

2. Depressurization events, including: opening of one control or turbine bypass valve.

3. Core flow transients do not apply to ESBWR, since the initiating event does not apply to a natural circulation BWR.

4. Cold water events, including: loss of feedwater heating and inadvertent Isolation Condenser injection.

5. Level transient events such as partial or complete loss of feedwater.

The preliminary list of AOOs for ESBWR in Table 4 Reference 20 was considered for determining the limiting ATWS scenario. This list has been finalized in the ESBWR DCD, and used for the ATWS section of the DCD. Any additions that may affect the limiting ATWS scenarios will be considered in the DCD. The ESBWR AOO events were considered in a screening process, to select the most limiting ATWS scenarios. The scenarios are grouped into three categories. The first category includes events that demonstrate ATWS mitigation for the most severe and limiting cases. The uncertainties involved in the analysis of these events will be quantified.

The second category has events that are less severe. Results are provided in the safety analysis to demonstrate they are bounded by the category I events, and show the sensitivity of key ATWS parameters. If a category II event is determined to be more severe than a category I event, an additional uncertainty evaluation will be provided.

The third category covers the cases that have only minor impact to the reactor vessel and containment. They are discussed briefly in the safety analysis report to justify that they do not significantly influence the design of ATWS mitigation. No calculations will be performed for events in the third category. The ATWS scenarios in each category are given below:

ESBWR ATWS Categorization

Abnormal Operational Occurrence	ATWS Severity	Category
Loss of Feedwater Heating	In ESBWR this event is mitigated with Select Control Rod Run-In (SCRRI). Consistent with ATWS failure to scram, this event will be evaluated with no SCRRI. This event is included in category I, to determine whether it will be limited for peak clad temperature. Because the turbine bypass valves are available, it is not limiting for vessel pressure or suppression pool temperature.	I

Abnormal Operational Occurrence	ATWS Severity	Category
Closure of One Turbine Control Valve	Because other TCVs and the bypass valves are available, the pressurization rate is less severe than MSIVC, and the energy addition to the pool is less severe than MSIVC.	III
Generator Load Rejection with Bypass	Because the bypass valves are available, the pressurization rate is less severe than MSIVC. The FW temperature change will be similar to MSIVC and the energy addition to the pool is less severe than MSIVC.	III
Generator Load Rejection with a Single Failure in the Turbine Bypass System	Because half of the bypass valves are available, the pressurization rate is less severe than MSIVC, the FW temperature change will be similar to MSIVC and the energy addition to the pool is less severe than MSIVC.	II
Turbine Trip with Bypass	Because the bypass valves are available, the pressurization rate is less severe than MSIVC, the FW temperature change will be similar to MSIVC and the energy addition to the pool is less severe than MSIVC.	III
Turbine Trip with a Single Failure in the Turbine Bypass System	Because half of the bypass valves are available, the pressurization rate is less severe than MSIVC, the FW temperature change will be similar to MSIVC and the energy addition to the pool is less severe than MSIVC. Because the Generator Load Rejection event with a single failure in the bypass system is similar and a category II event, it's evaluation will address the severity of turbine trip with a single failure in the turbine bypass, and the turbine trip event can be category III.	III
Closure of One Main Steam Isolation Valve	Because the three main steam lines are available, the pressurization rate is less severe than MSIVC, and the energy addition to the pool is less severe than MSIVC.	III
Closure of All Main Steam Isolation Valves (MSIVC)	Generic studies have shown that this transient produces high neutron flux, heat flux, vessel pressure, peak cladding temperature, and suppression pool temperature. The maximum values from this event are, in most cases, bounding of all events considered.	I

Abnormal Operational Occurrence	ATWS Severity	Category
Loss of Condenser Vacuum	The turbine will trip on low condenser vacuum. The bypass valves are available for a short period, and then close on low condenser vacuum. Depending on detailed BOP performance the pressurization rate and the energy addition to the pool may be as severe as MSIVC. This event is included in category I to assure the short term peak vessel pressure and clad temperature remain within limits.	I
Loss of Shutdown Cooling Function of RWCU/SDC System	When the reactor is at power, other heat sinks besides RWCU/SDC are available. Loss of RWCU/SDC is only a concern when the reactor is subcritical.	III
Inadvertent Isolation Condenser Initiation	Spurious initiation of the isolation condensers would cause a moderator temperature decrease and a slow insertion of positive reactivity into the core. During power operation, the system will settle at a new steady state.	II
Runout of One Feedwater Pump	The other FW pumps will reduce flow to compensate for the runout pump. This event is expected to be bounded by Loss of Feedwater Heating with SCRRI failure.	III
Opening of One Control or Turbine Bypass Valve	This event assumes a hydraulic system failure that causes a mild decrease in pressure, which is compensated by the control system closing other valves. The ATWS response will not be limiting.	III
Loss of Unit Auxiliary Transformer	The event is expected to result in a fast transfer of the buses and no scram or pressurization.	III
Loss of Grid Connection	The response is similar to Load Rejection with bypass.	II

Abnormal Operational Occurrence	ATWS Severity	Category
Loss of All Feedwater Flow	Initially this will cause a reduction in reactor power and pressure. This transient is less severe than the category I events, because the initiating event is one of the ESBWR ATWS mitigation features, FW reduction, which reduces core power. Following MSIVC closure at low water level, there will be pressurization that is bounded by the MSIVC ATWS. The energy addition to the pool is less severe than MSIVC, because of the initial power reduction. It is the only event that is mitigated by ARI or FMCRD run-in initiated from the low level signals. It is analyzed in the DCD to show that the low level trips are capable of mitigating the event.	II

[[Proprietary Information Redacted]]

A detailed description of these three events is given in Section 8.

2.9 Nuclear Power Plant Selection

The included plant type is ESBWR.

3.0 PHENOMENA IDENTIFICATION AND RANKING TABLES (PIRT)

The critical safety parameters, for ESBWR ATWS analyses, are reactor pressure vessel (RPV) pressure, peak fuel clad temperature (PCT), containment pressure and suppression pool temperature. These are the criteria used to judge the performance of the safety systems and the margins in the design. The values of the critical safety parameters are determined by the governing physical phenomena. To delineate the important physical phenomena, it has become customary to develop phenomena identification and ranking tables (PIRTs). PIRTs are ranked with respect to their impact on the critical safety parameters. For example, the vessel pressure is determined by the reactor short-term response to an ATWS. The coupled core neutronic and thermal-hydraulic characteristics and the response of mitigation systems govern the vessel pressure, clad and suppression pool temperature transients.

All processes and phenomena that occur during an ATWS do not equally influence plant behavior. The most cost efficient, yet sufficient, analysis reduces all candidate phenomena to a manageable set by identifying and ranking the phenomena with respect to their influence on the critical safety parameters. The phases of the events and the important components are investigated. The processes and phenomena associated with each component are examined. Cause and effect are differentiated. After the processes and phenomena have been identified, they are ranked with respect to their effect on the critical safety parameters for the event.

The phenomena identification and ranking tables (PIRTs) represent a consensus of GE expert opinions. PIRTs are developed with only the importance of the phenomena in mind and are independent of whether or not the model is capable of handling the phenomena and whether or not the model will show a strong sensitivity to the phenomena. For example, two phenomena may be of high importance yet tend to cancel each other in many AOO transient events so that there is little sensitivity to either phenomenon. Both phenomena would be ranked as high importance because the balance between these competing phenomena is important.

Table 3-1 was developed to identify the phenomena that govern ESBWR ATWS responses. In ranking the phenomena, it is helpful to divide the limiting scenarios into phases. The following five phases are defined in an ESBWR ATWS:

1) Short term pressurization, neutron flux increase, and fuel heatup. This phase is similar to the forced circulation plants. Void and Doppler reactivity feedback limit the power increase. Safety valve opening limits the vessel pressure. The important phenomena and uncertainties are the same as References 1, 8 and 13.

2) Feedwater runback, water level reduction. This phase is similar to the forced circulation plants. Water level reduction reduces the reactor power. The important phenomena and uncertainties are the same as References 1 and 13.

3) Boron injection, mixing and negative reactivity insertion. This phase includes phenomena which were previously included in the Reference 13 PIRT, and applies TRACG boron transport models described in Reference 14.

4) <u>Post Shutdown Suppression Pool Heatup.</u> The phenomena involved in this phase are limited to those that affect decay heat and cooling of the suppression pool. The ranking of other phenomena, which do not occur in this phase are left blank. This phase is of limited importance in ESBWR, because the Isolation Condenser is able to terminate steam flow to the pool once the core is subcritical.

5) <u>Depressurization of the reactor.</u> Although the ESBWR EOPs have not been developed at this time, they may direct the operator to depressurize the reactor during an ATWS, and this is considered ESBWR ATWS analysis. If the suppression pool is calculated to reach the heat capacity temperature limit, the energy added to pool by manual SRV opening is included in the analysis. The important phenomena and uncertainties are the same as References 1 and 13.

For each event type, the phenomena are listed and ranked for each major component in the reactor system. The ranking of the phenomena is done on a scale of high importance to low importance or not applicable, as defined by the following categories:

- *High importance (H):* These phenomena have a significant impact on the primary safety parameters and should be included in the overall uncertainty evaluation. An example of such a parameter would be the *void coefficient* during the short term pressurization phase (C1AX in Table 3-1). The void coefficient determines the amount of reactivity change due to void collapse during this phase.

- *Medium importance (M):* These phenomena have insignificant impact on the primary safety parameters and may be excluded in the overall uncertainty evaluation. An example of such a parameter would be the *direct moderator heating* during the pressurization, level reduction and boron injection phases (C3DX in Table 3-1). Direct moderator heating deposits some of the core energy in the in-channel and bypass moderator in the initial steady state and during the transient. Its modeling can be expected to have some effect on the results, but the critical safety parameter will not be highly sensitive to modeling uncertainty in this phenomenon

- *Low importance (L) or not applicable (N/A):* These phenomena have no impact on the primary safety parameters and need not be considered in the overall uncertainty evaluation. An example of such phenomena would be *Steam Dome Condensation On Walls* during the pressurization phase of an ATWS (K2 in Table 3-1). The maximum energy that could be absorbed in the steam dome metal, is a small fraction of the core power, and it could not impact the critical parameters in any significant way.

The PIRT serves a number of purposes. First, the phenomena are identified and compared to the modeling capability of the code to assess whether the code has the necessary models to simulate the phenomena. Second, the identified phenomena are cross-referenced to the qualification basis to determine what qualification data are available to assess and qualify the code models and to determine whether additional qualification is needed for some phenomena. As part of this assessment, the range of the PIRT phenomena covered in the tests is compared with the corresponding range for the intended application to establish that the code has been qualified for the highly ranked phenomena over the appropriate range.

Finally, uncertainties in the modeling of the highly ranked PIRT phenomena are carefully evaluated, and then combined through a statistical process, to arrive at the total model uncertainty. In this third stage, one may find that some highly ranked phenomena do not contribute significantly to the overall uncertainty even when conservative values for the individual phenomena uncertainties are used. It is at this stage that one can determine how individual uncertainties influence the total uncertainty so that the effort can be focused on establishing the uncertainties for those phenomena that have the greatest impact on the critical safety parameters. These uncertainties will be more fully developed later in this report and their impact on the critical safety parameters will be quantified for each of the transient scenarios.

Phenomena involved in each phase are included in the PIRT. The phenomenon identification and ranking process for ESBWR involved reviewing the PIRTs in References 1, 8 and 13. The definitions of the PIRT parameters are provided in Reference 13, supplement 1. For ESBWR ATWS evaluation, the following specific definitions are employed:

ATW1 Boron mixing/entrainment between the jets downstream of the injection nozzle.

ATW2 Boron settling in the guide tubes or lower plenum.

ATW3 Boron transport and distribution through the vessel, particularly in the core bypass region.

Table 3-1. Phenomena That Govern ESBWR ATWS Response

[[Proprietary Information Redacted]]

4.0 APPLICABILITY OF TRACG TO ATWS ANALYSES

The objective of this section is to demonstrate the applicability of TRACG for the analysis of anticipated transient without scram events in ESBWR. To accomplish this purpose, the capability of the TRACG models to treat the highly ranked phenomena and the qualification assessment of the TRACG code for ATWS applications is examined in the next two subsections

4.1 Model Capability

The capability to calculate an event for a nuclear power plant depends on four elements:

- Conservation equations, which provide the code capability to address global processes.

- Correlations and models, which provide code capability to model and scale particular processes.

- Numerics, which provide code capability to perform efficient and reliable calculations.

- Structure and nodalization, which address code capability to model plant geometry and perform efficient and accurate plant calculations.

Consequently, these four elements must be considered when evaluating the applicability of the code to the event of interest for the nuclear power plant calculation. The key phenomena for each event are identified in generating the PIRTs for the intended application, as indicated in Section 3. The capability of the code to simulate these key phenomena is specifically addressed, documented, and supported by qualification. [11, 15]

Important BWR phenomena have been identified and TRACG models have been developed to address these phenomena as indicated in Table 4.1-1.

Table 4-1. ESBWR Phenomena and TRACG Model Capability Matrix

[[Proprietary Information Redacted]]

4.2 Model Assessment Matrix

The qualification assessments of TRACG models are summarized in Table 4.2-1. The models are identified so that they may be easily correlated to the model description and qualification reports. For each model, the relevant elements from the Model Description LTR [14] and the Qualification LTRs [11, 15] are identified.

For each of the governing BWR phenomena, TRACG qualification has been performed against a wide range of data. In this section, the qualification basis is related to the phenomena that are important for the intended application. This is a necessary step to confirm that the code has been adequately qualified for the intended application.

The complete list of phenomena is cross-referenced to the model capabilities in Reference 14. Similarly, as shown in References 11 and 15, the complete list of phenomena is cross-referenced to the qualification assessment basis. Data from separate effects tests, component tests, integral system tests and plant tests as well as plant data have been used to qualify the capability of TRACG to model the phenomena.

.

Table 4-2. Qualification Assessment Matrix for ESBWR ATWS Phenomena

[[Proprietary Information Redacted]]

5.0 MODEL UNCERTAINTIES AND BIASES

The model biases and uncertainties for all items from the PIRT table (Table 3-1), which have been identified as having a significant impact on the limiting ATWS scenario, have been evaluated. In Section 5.1, overall model biases and uncertainties for the ATWS application are assessed for each high ranked phenomenon.

The Effect of Nodalization and Effect of Scale is described in Section 5.2 and 5.3.

The uncertainty screening results for the Main Steam Isolation Valve Closure ATWS (MSIVC) event are shown in Section 8.3.1.1.

5.1 Model Parameters and Uncertainties

This section discusses the uncertainties associated with each item that has been ranked High for some phase of the ATWS scenario. Past practice has been to evaluate all High and Medium ranked parameters. 31 parameters were ranked High in Table 3.1-1 and 32 were ranked Medium for a total of 63 parameters. Previous experience has shown that the Medium parameters rarely have any impact on the results and serve to dilute the identification of the truly significant parameters. In fact, it is expected that only a half dozen or so of the High ranked parameters will demonstrate any significant sensitivity. Hence this study is restricted to the High ranked parameters. A few of the Medium ranked parameters are also perturbed in Section 8 to show that they have no impact. An estimate of bias and uncertainty for each parameter was obtained by using a combination of comparisons of calculated results to: (1) separate-effects test facility data, (2) integral test facility test data, (3) component qualification test data and (4) BWR plant data. Where data are not available, cross-code comparisons or engineering judgment are used to obtain approximations for the biases and uncertainties. For some phenomena that have little impact on the calculated results, it is appropriate to simply use a nominal value or to conservatively estimate the bias and uncertainty. Table 5.1-2 provides the dispositions of the high ranked ATWS model parameters from Table 4-2. The ID and description are listed for each item.

ATW1 Boron Mixing in the Bypass

The Standby Liquid Control System (SLCS injection is through a header located near the top of the ESBWR downcomer. From the header, spaced equally around the downcomer, are four feeder pipes each of which has four nozzles at different elevations. Each nozzle extends through the shroud wall so that the nozzles discharge directly into the peripheral region of the bypass. The discharge elevations of the nozzles from the four feeder pipes are the same. The lowest injection point is 0.25m above the bottom of the active fuel and the three sets of higher nozzles are spaced at 0.4m intervals. The uppermost nozzle in each of the four banks is approximately at mid-core height (1.45m). Each nozzle has two discharge ports, so the injected liquid forms two jets, pointing at angles estimated to be 60 degrees on either side of a line through the nozzle centerline to the core center and in a horizontal plane at the elevation of the nozzle (Figure 5.1-1).

<u>Movement of Injected Borated Solution through the Bypass Region</u>

The borated solution emerges from the injection nozzles as high velocity jets. The discharge velocity from the nozzles is of the order of 34 m/s. The borated solution is at a much lower

temperature than the ambient fluid in the bypass region. Consequently, the density of the injected solution is approximately 40% higher than the bypass water. Note that the density of the sodium pentaborate salt is not a major factor at the salt concentrations in the injected solution; the density difference is almost entirely due to the difference in the density of water at the lower temperature. The specific gravity of the injected solution is 1.065, relative to a water specific gravity of 1.0 at 18 °C.

The jets will traverse the annular space that constitutes the peripheral bypass region and impinge on the peripheral channels. Because of the density difference, the jets may also move downwards, but the horizontal velocities, being much larger, will be predominant. Figure 5.1-2 shows a schematic of the cross-section at an injection elevation. By the time the jet reaches the channel boundary, the jet will have entrained a substantial amount of ambient fluid and slowed down to a velocity of about 2 m/s and warmed up to within about 13 °C of the bypass ambient fluid. The impinging jet will begin to spread sideways and towards the shroud wall (as indicated in the figure by the backward arrows) but the complex geometry due to the channel walls will likely prevent it from spreading extensively.

(For this analysis a jet angle with respect to the nozzle of 60 degrees was assumed. If the angle is greater and the jet is closer to the shroud wall, it could attach itself to the wall. This jet reattachment behavior is called the Coanda effect and has been observed in jets near solid boundaries [36]. This would result in even more mixing and dilution of the SLCS jet, which would adhere to the shroud wall and carry around until it encountered the wall jet from the adjacent nozzle. However, no credit will be taken for a potential Coanda effect in this analysis.)

As the jet impinges on the channel wall, the heavier solution will tend to sink downwards in the gap between the channels and the shroud wall. The movement of this plume will be affected by the fluid velocity in the bypass. A sufficiently large upward velocity could carry the plume upwards. However, the TRACG results show that the vertical velocity in the bypass prior to boron injection is close to zero and slightly negative. This will result in negatively buoyant downward plumes. The plumes sinking from the top injection point will interact with those directly below and reach the bottom of the bypass with a small density surplus relative to the ambient fluid. The path of these plumes is sketched in Figure 5.1-3. The plumes are not likely to spread significantly in their descent and will be confined to fairly narrow regions, one in each quadrant corresponding to the four nozzle locations along the periphery of the core shroud.

Having reached the bottom of the bypass, the borated solution (considerably diluted by this point) will spread peripherally and radially inwards along the top of the core support plate. As it spreads, the borated solution will move over guide tube openings (left side of Figure 5.1-4). Some of the solution could sink into the guide tubes and be lost from the viewpoint of achieving shutdown of the nuclear fission reaction in the core. The bulk of the boron will make its way into the fuel channels through the leakage holes in the lower tieplates of the fuel channels. The peripheral fuel bundles could have a downward velocity at the inlet. If so, the boron entering these channels will move downwards into the lower plenum. This boron will re-enter the core when the flow velocities at the top of the lower plenum are upwards. The boron that enters the central channels will move upwards into the fuel bundles, carried up by the upward velocities in these bundles. Boron in the bypass as well as that in the fuel channels results in negative reactivity and the desired shutdown of the fission reaction.

The flow regimes discussed above are pieced together in a more quantitative manner in the following paragraphs.

<u>Initial Jet Regime</u>

Figure 5.1-1 is a schematic showing the nozzle location in the shroud wall and the approximate location of the outer boundary of the fuel channels. The channel boundary is based on a channel pitch of 15.5 cm and there are 19 channels from the core center to the periphery on four sides. This may underestimate the channel boundary at some locations but applies on the 90 degree sector boundaries. With a jet angle estimated to be 60 degrees on either side of the nozzle centerline, the distance along the jet centerline from the shroud wall to the channel boundary is estimated to be about 0.5m, or over 80 diameters, using a 6 mm initial jet diameter. The characteristics of the circular turbulent submerged jet are summarized by the empirical equations given below [36]. These are time-averaged properties of the turbulent jet, based on experimentally measured coefficients. The equations apply to the 'fully developed' region of the jet, that is the axial distance from the discharge point must be greater than the length of the initial region, xi

Circular Turbulent Jet Characteristics [36, Table 9-3, p 236]

Length of initial region, x_i	$10\ r_0$
Centerline Velocity, u_m	$12\ (r_0/x)\ U_0$
Velocity Profile, u/u_m	$\exp[-94\ (r/x)^2]$
Width, b (where $u/u_m = 0.5$)	$0.086\ x$
Volume flow rate, Q	$0.16\ (x/r_0)\ Q_0$
Centerline Temperature Deficit, ΔT_m	$10\ (r_0/x)\ \Delta T_0$
Temperature Deficit Width, $b_{\Delta T}$ (where $\Delta T/\Delta T_m=0.5$)	$0.11\ x$
Temperature Deficit Profile, $\Delta T/\Delta T_m$	$\exp[-57\ (r/x)^2]$

where: x – distance along jet centerline

 r – jet radius at x

 r_0 – initial jet radius

 u_m – jet centerline velocity at x

 ΔT_m – jet centerline temperature deficit at x

 U_0 – jet initial velocity

 ΔT_0 – jet initial temperature difference relative to the ambient temperature

 $= T_{bypass} - T_0$, where T_0 is the injection temperature (18 °C) and T_{bypass} is the bypass temperature (300 °C) at the time SLCS injection begins based on TRACG calculations (Figures 5.1-5 and 5.1-6).

These equations have been derived assuming fluid at an ambient temperature T_{bypass} is drawn into the mixing region, but the density difference corresponding to the different temperature is not accounted for in the mass and momentum balances. Hence, this solution must be considered approximate when there are large differences between the injected and ambient densities. Accordingly, we use only the expression for the entrained volume of ambient liquid, but calculate the temperatures and densities using mass and energy balances.

Applying the above equations,

At jet discharge,

$r_0 = 0.003$ m
$A_0 = \pi r_0^2 = 2.827e\text{-}5$ m^2
$U_0 = 34.2$ m/s
$Q_0 = U_0 A_0 = 0.000967$ m^3/s

At channel outer boundary (x = 0.5m)
$u_m = 2.46$ m/s
$Q_{ch} = 0.026$ m^3/s

This suggests that the centerline velocity of the jet will be reduced by a factor of over 12 and the fluid entrained will decrease the temperature deficit at the jet centerline by a large factor. Because the jet fluid is also heavier than the surrounding fluid, the jet will likely droop, resulting in longer distance between the discharge and the channel boundary. Reference 36 provides criteria for determining if a buoyant jet will behave like a jet or like a buoyant plume. For jet-like behavior, the distance along the jet should be less than:

$X_j < \Pi_o^{3/4}/B^{1/2}$

where

Π_o = initial jet specific momentum = $A_0 U_0^2$
B_0 = specific buoyancy flux = $Q_0 g (\rho_0 - \rho_{bypass})/\rho_{bypass}$
A_0 = initial jet area
ρ_0 = density of injected fluid
ρ_{bypass} = density of bypass inventory

Using typical values for the injected liquid density of 1058 kg/m3 and bypass water density at 300 °C of 712 kg/m3 and the jet properties from the above relations, X_j becomes about 1.14m, so the jet should retain jet-like behavior to the channel boundary.

Plumes with Negative Buoyancy

The jet impinging on the channel wall will try to spread in a plane normal to the incident jet, i.e. the plane of the channel wall. Horizontal spreading is restricted by the adjacent channels and the shroud wall, and upward spreading is limited by negative buoyancy effects. It is assumed that a well-mixed region will result from the termination of each jet, which is the source for a vertical plume with negative buoyancy. The size of this region is of the order of a channel width. The properties of this well-mixed region are calculated by averaging the jet conditions at the channel boundary.

$M_0 = Q_0 {}^* \rho_0$
$M_{induced} = (Q_{ch} - Q_0)^* \rho_{Bypass}$
$M_{total} = M_0 + M_{induced}$
Designating enthalpy by h,
$h_{ave} \sim (M_0 {}^* h_0 + M_{induced} {}^* h_{bypass})/M_{total}$
$T_{ave} = 287.3$ °C
$\rho_{ave} = 737$ kg/m^3
Average temperature deficit = $\Delta T_{ave} = 13$ °C

First, we check for the effects of the bypass vertical velocity.

A modified Froude number can be calculated based on the hydraulic diameter of the peripheral bypass (twice the effective gap = 0.453 m), the average vertical velocity in the peripheral bypass (calculated by TRACG just prior to boron injection), and the density difference between the plume and the bypass ambient liquid.

$$Fr = \frac{\rho V^2}{g \Delta \rho D_h}$$

Generally, the Froude number must be of the order of 1 to cause the plume to be carried upwards. Experimental evidence exists in the form of tests for counter current flow limiting (CCFL) with gas–liquid flows. Tests have been performed in large downcomers with upward flow of a light species (gas) and downward flow of liquid. Downward liquid penetration was shut off when the square root of the gas Froude number is of the order of 0.14 [14].

If we assume a similar critical Froude number for the situation of liquid/liquid countercurrent flow, the critical upward velocity given by:

$$V_{crit} = 0.14 * \sqrt{(\Delta \rho / \rho) g D_h} = 0.055 \quad m/s$$

The velocity in the bypass region calculated by TRACG is downwards. Therefore, the plumes will descend in the gap between the outer channels and the core shroud.

Spreading of Downward Plumes

Each set of nozzles produces a plume that starts descending in the peripheral bypass to the core plate. The plume behaves more like a submerged jet at smaller distances from the sources. A minimum distance can be calculated beyond which plume spreading can be assumed.

This distance is given by:

$$X_j = \Pi^{3/4} / B^{1/2}$$

where

        B = specific buoyancy flux = $Q_{ch} g (\rho_{ave} - \rho_{bypass})/\rho_{bypass}$
        where Q_{ch} is the initial volumetric flow source for the plume, taken as the flow carried in by the turbulent submerged jet with an initial mixed density ρ_{ave}.
        Π = initial plume specific momentum = $Q_{ch} U_{ch}$
        Π is estimated as follows:
        By conservation of momentum, $(\rho_{ave} U_{ch}^2 A_{ch}) \sim (\rho_0 U_0^2 A_0)$
        $\Pi = (U_{ch}^2 A_{ch}) = (\rho_0 U_0^2 A_0)/ \rho_{ave}$
        $X_j = \Pi^{3/4} / B^{1/2} = 1.08m$

The calculations based on a plume are valid only for distances greater than 1.08m. For distances shorter than 1.08m, it will be assumed that the plume has not spread or mixed further with the ambient fluid.

Circular Plume Characteristics [36, Table 9-7, p 250]

Centerline Velocity, u_m	$3.5\,B^{1/3}\,x^{-1/3}$
Axial Velocity Profile, u/u_m	$\exp[-57\,(r/x)^2]$
Width, b (where $u/u_m = 0.5$)	$0.11\,x$
Volume flow rate, Q	$0.15\,B^{1/3}\,x^{5/3}$
Centerline Temperature Deficit, ΔT_m	$11\,(Q_{ch}\,\Delta T_{ave})\,B^{-1/3}\,x^{-5/3}$
Temperature Deficit Width, $b_{\Delta T}$ (where $\Delta T/\Delta T_m = 0.5$)	$0.10\,x$
Temperature Deficit Profile, $\Delta T/\Delta T_m$	$\exp[-69\,(r/x)^2]$

If the plumes from the four different elevations are assumed not to interact with each other, the volumetric flow rates in the plumes when they reach the bottom of the bypass can be calculated from the above table.

Only the top plume source is more than 1.08m from the bottom of the bypass. The lower plumes are assumed not to spread. The plume flow and average temperatures when they reach the core plate are calculated as below:

The volumetric flow rate Q_P is evaluated from Row 4 of the above table for x >1.08m. For x < 1.08m, it is assumed flow is not entrained from the bypass and the initial plume flow reaches the core plate.

1. $x = 1.45\text{m}$, $Q_{P1} = 0.058\ \text{m}^3/\text{s}$
2. $x = 1.05\text{m}$, $Q = 0.026\ \text{m}^3/\text{s}$
3. $x = 0.65\text{m}$, $Q = 0.026\ \text{m}^3/\text{s}$
4. $x = 0.25\text{m}$, $Q = 0.026\ \text{m}^3/\text{s}$

The total source from the four elevations is 0.136 m3/s. The average temperature deficit is calculated as before through an energy balance:

$$M_{ch} = 4*M_{jet} = 4*18.7$$
$$M_{induced} = (0.136-4*0.026)*\rho_{bypass}$$

$$T_P = (M_{ch}*T_{ave}+M_{induced}*T_{bypass})/M_{total} = 290.2\ ^0C$$
$$\Delta T_P = 10\ ^0C.$$

The corresponding density difference relative to the ambient fluid ($\Delta\rho/\rho$) is 0.027.

These sources of borated solution will spread peripherally and radially at the bottom of the bypass.

Settling of Boron into Guide Tubes

The possibility of boron settling into the guide tubes is evaluated by calculating the critical velocity at the top of the guide tubes that will prevent settling. The critical velocity is based on a corresponding critical Froude number. Analogy with CCFL data at similar locations shows that the square root of the Froude number for shutoff of downflow is of the order of 0.5 to 0.6, though values as high as 1 are possible with sharp edged openings [37].

Using a limiting value of 1 yields a critical velocity of:

$$V_{crit} = 1.0 * \sqrt{(\Delta\rho/\rho)gD_h}$$

For a temperature deficit of 10 °C, $\Delta\rho/\rho$ is 0.027. The hydraulic diameter for the guide tube opening is approximately 1 cm.

$$V_{crit} = 0.05 \text{ m/s}$$

Thus, velocities of the order of 5 cm/s at the top of the guide tubes should prevent any settling of boron into the guide tubes.

Settling of Boron into the Lower Plenum from the Channel Inlet Nosepieces

Boron enters the bottom of the fuel channels with the leakage flow through leakage paths between the bypass and the fuel bundles. The largest leakage path consists of holes drilled in the lower tieplate (right hand side of Figure 5.1-4). If flow is draining through the lower nosepiece of the tieplate, the boron will travel with this flow into the lower plenum. If the inlet velocity at the nosepiece is large and upward, the boron will tend to move up with the flow into the active fuel region. In a range of velocities between zero and a critical upward velocity, boron could settle downwards due to the density difference between the borated solution and the ambient liquid in the inlet region. TRACG would not calculate this settling behavior and would therefore be non-conservative in this range of velocities. The critical velocity is calculated as before through a critical Froude number.

$$V_{crit} = 1.0 * \sqrt{(\Delta\rho/\rho)gD_h}$$

The leakage flow enters the channel inlet region through small leakage paths, with the dominant path being two 7 mm holes in the wall of the inlet nosepiece. About 40% of the flow comes through leakage paths between the tieplate and the channel box, with clearances of the order of 1 mm. An area-averaged path size of 3 mm was calculated for the leakage flow. The inlet temperature of the jets is assumed to be the temperature of the boron plumes at the core plate. The temperature inside the nosepiece is assumed to be the same as the bypass temperature of 300 C. Typical velocities for the leakage jets are of the order of 1 to 2 m/s. Jet like behavior will persist for

$$X_j < \Pi_o^{3/4}/ B^{1/2}$$

where

Π_o = initial jet specific momentum = $A_0U_0^2$
B_0 = specific buoyancy flux = $Q_0 g (\rho_0 - \rho_{LTP})/\rho_{LTP}$
$X_j < \Pi_o^{3/4}/ B^{1/2} = 0.12$ m

Thus, the entering leakage will travel as jets for approximately 4 cm to the center of the nosepiece. Using the formula for circular jets from Section 3 above,

$$Q = 0.16 (x/r_0) Q_0 = 4.26 Q_0$$

and the temperature deficit is reduced by this factor to (300-290.2)/4.26=2.3 °C.

Thus, the temperature deficit of 10 C at the bottom of the bypass is reduced to approximately 2.3 °C by mixing within the nosepiece. For a temperature deficit of 2.3 °C, $\Delta\rho/\rho$ is 0.0065. The hydraulic diameter for the lower tieplate opening is approximately 8 cm.

$$V_{crit} = 0.07 \text{ m/s}$$

Thus, velocities of the order of 7 cm/s at the inlet to the fuel bundle should prevent any settling of boron into the lower plenum.

In the peripheral bundles, the flow through the lower tieplates is downwards. Hence, the borated flow through the leakage paths is carried down into the lower plenum. The borated flow enters with a density differential of 0.027. It is further considerably diluted by the downward flow of saturated water through the bundle. Thus the flow discharging from the side entry orifices into the lower plenum will be well mixed and essentially at saturation temperature. Further consideration of stratification within the lower plenum is not required.

Change in Bypass Temperature during the ATWS Transient

The SLCS jets discharging into the peripheral bypass entrain large amounts of ambient fluid from the peripheral bypass region. As the transient progresses, the average temperature of the bypass fluid feeding the jets will change. In order to account for the transient history, results of the TRACG analysis were examined. The flow in the bypass region is downward through this phase of the transient. Flow leaving the bypass through the leakage holes in the channels is replaced by downflow from the upper plenum. Figures 5.1-5 and 5.1-6 show the temperature history in the bypass region during an ATWS event. Here Level 5 is the SLCS injection level (all four elevations are within Level 5) and Level 7 is above the injection location. At the time of boron injection (~200 s), the bypass temperatures are uniform and close to 573 K (300C). Shutdown by boron is achieved before 400 s. During this period, the temperature in the upper level, which is the upstream region away from the immediate vicinity of the jets, drops by less than 1C. Level 5 shows a bigger drop (~15 C in the sectors where boron is injected) because TRACG calculates the mixed temperature with the colder borated solution. However, it is reasonable to assume that the liquid entrained by the jets from the bypass is closer in temperature to that in Level 7. Hence, no changes are needed in the current analysis to track the temperature history in the bypass ambient temperature.

Implications for TRACG Analysis

[[Proprietary Information Redacted]]
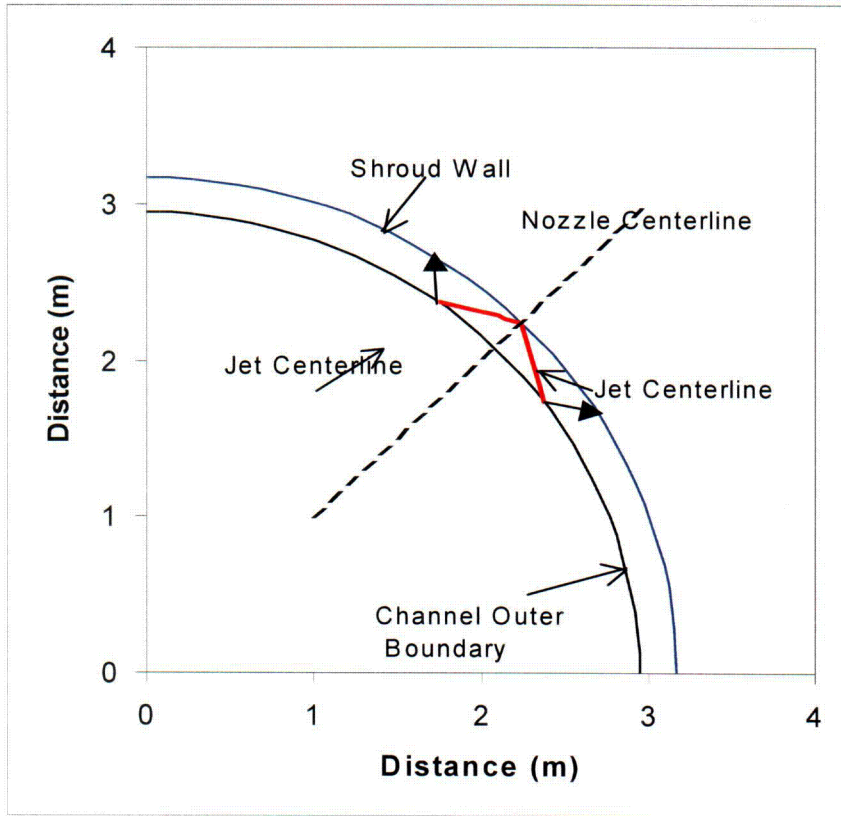
Figure 5.1-1. Overall geometry of Injected jets and peripheral Bypass

C01
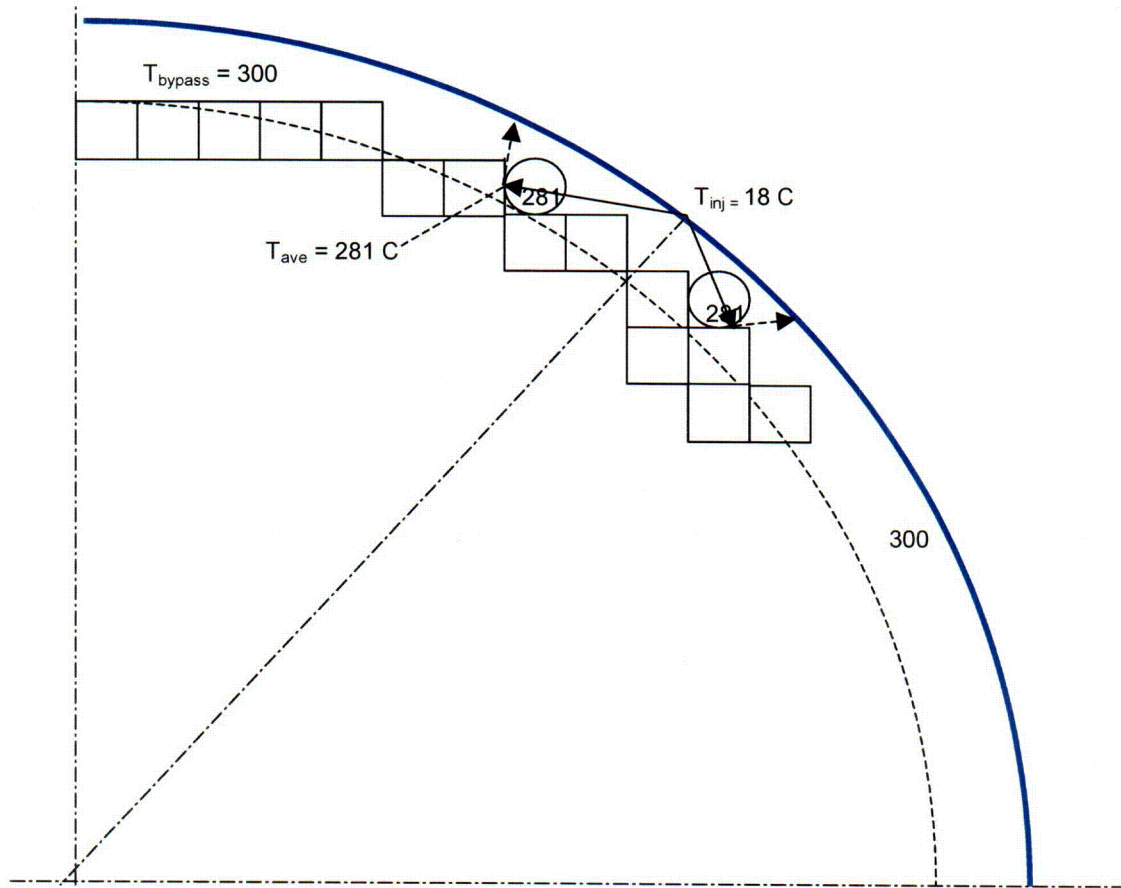
Figure 5.1-2. Channel Geometry and Jet Properties in Cross-section of Injection Locations
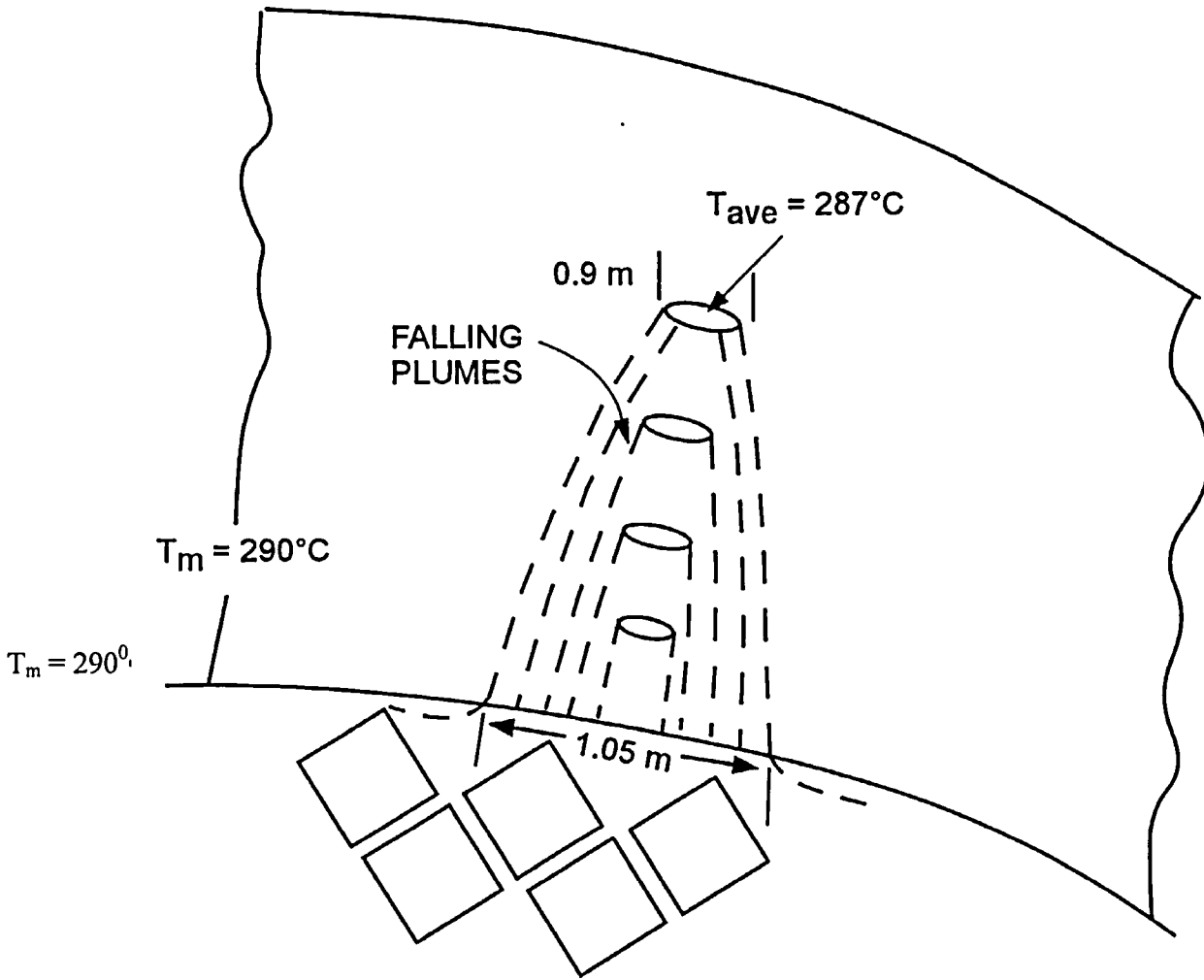
Figure 5.1-3. Downward Plumes in Annular Space
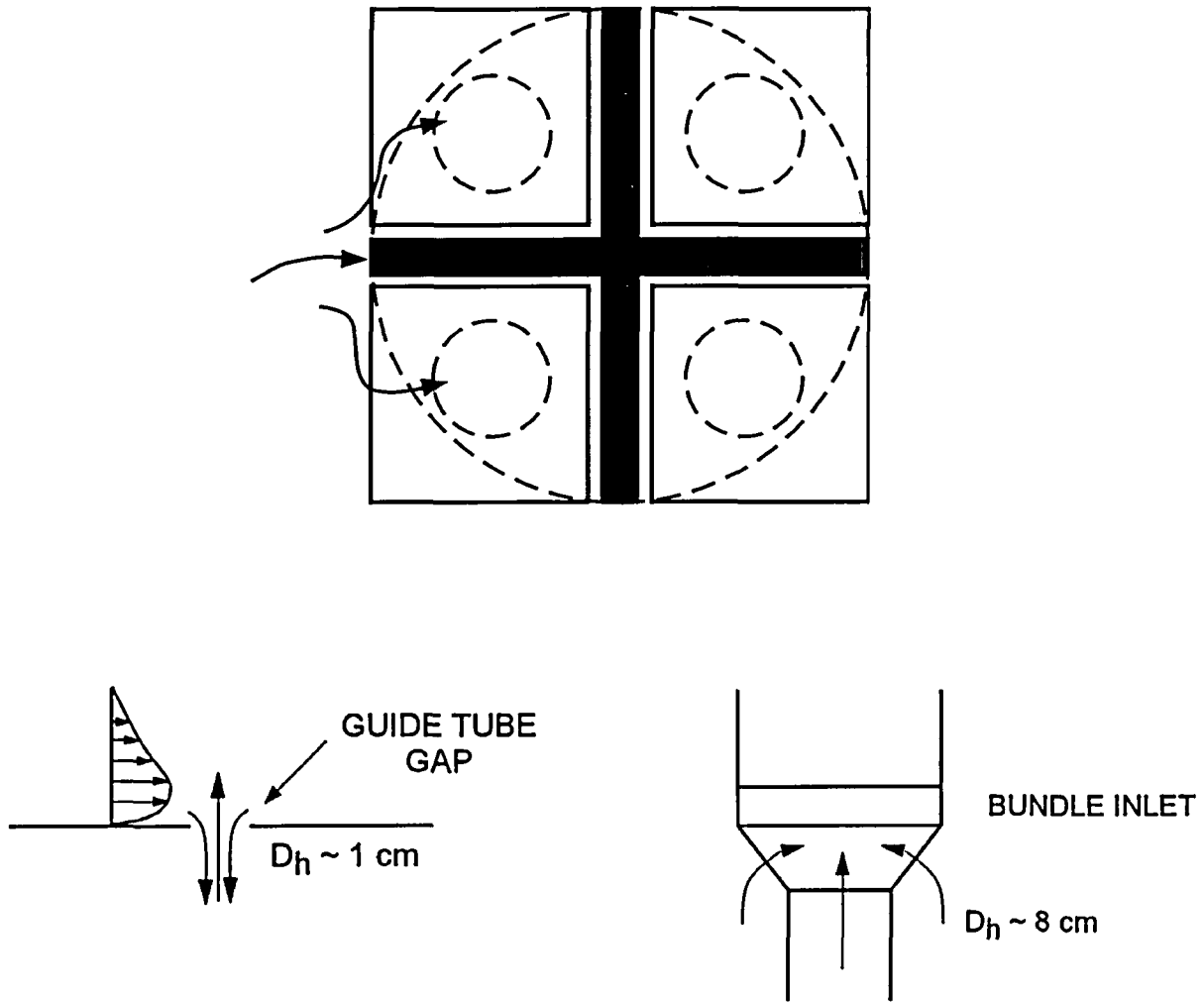
Figure 5.1-4: Boron settling in guide tubes and lower plenum

[[Proprietary Information Redacted]]

Figure 5.1-5: Liquid temperatures calculated in the bypass region by TRACG at Level 7 (above injection elevation)

[[Proprietary Information Redacted]]

Figure 5.1-6: Liquid temperatures calculated in the bypass region by TRACG at Level 5 (Injection Elevation)

B1   Bypass Flashing

Bypass flashing is controlled by liquid-side interfacial heat transfer in the TRACG model. The bubbly flow regime is the dominant flow regime for this behavior. TRACG uses the Lee-Ryley correlation in conjunction with a bubble diameter based on a critical Weber number for liquid-side heat transfer in the bubbly flow regime [14]. The Lee-Ryley correlation applies to heat transfer to spherical particles under forced circulation conditions. It predicts the water droplet evaporation data from which it was originally developed with an error less than 10%. There are no experimental data for direct evaluation of the accuracy of the TRACG models for calculation of liquid-side interfacial heat transfer. Following the procedure previously adopted for the AOO application [12], the uncertainty in the PIRT multiplier on the interfacial heat transfer at the bubble surface is specified as a log-normal probability distribution with a mode of 1 and a gain of 2. This distribution has a standard deviation of 0.25 and imposes an effective cutoff on the multiplier at the extreme values of 0.5 and 2.

ATW3   Boron Transport to Core

See ATW1 discussion.

ATW5   Boron Reactivity

Boron reactivity is modeled in TRACG04 with the assumption that the removal of neutrons in the thermal energy group by B10 can be superposed in an unborated neutron flux spectrum on the other neutron removal mechanisms that are present. The B10 total neutron cross-section is modeled by a $1/v$ relationship, which provides an excellent approximation to the B10 thermal neutron absorption. In comparison, the B11 neutron absorption cross-section is negligible over the neutron energy range of interest. The expression for the boron absorption cross-section accounts for the effects of fuel temperature and self-shielding by the boron. In order to support the model development, boron cross-sections were evaluated with the GE lattice physics model (TGBLA06) [[Proprietary Information Redacted]]The results showed that the B10 cross-sections were not sensitive to the void history and that the TRACG modeling error had a weak dependence on the exposure, boron concentration and fuel temperature. Based on these comparisons, the uncertainty in the boron cross-section was estimated to be of the order of [[Proprietary Information Redacted]]. The lattice calculations do not capture the effect of change in neutron spectrum with voids, but the consistency in the model predictions indicate that the $1/v$ model will capture the effect of the neutron spectrum.

C1AX   Void Coefficient

[[Proprietary Information Redacted]]

Figure 5.1-7. TGBLA06 Void Coefficient Relative Bias and Relative Standard Deviation for Various Exposures (GWd/MT)

C1BX   Doppler Coefficient

TRACG uses a 3-D neutron kinetics model based on the PANACEA [21] neutronic parameters. Fuel temperature affects resonance absorption in uranium and plutonium. This is accounted for by the Doppler coefficient modifying the reactivity for each node. The 1σ uncertainty in the Doppler coefficient is [[Proprietary Information Redacted]] [5].

C1DX   3-D Kinetics and Power Shape

TRACG has a 3-D neutron kinetics model, based on the PANACEA formulation [21]. The TRACG kinetics model has been qualified against stability data for various BWRs, viz. LaSalle 2, Leibstadt. Steady-state power distribution comparisons have been made with data from several plants [11] and PANACEA predictions. The uncertainty of the kinetics model is determined by the uncertainty in scram reactivity, void and Doppler coefficient. For ATWS evaluations, the scram reactivity is not relevant.

C2AX   Interfacial Shear

Although this PIRT phenomenon is entitled "Interfacial Shear", it more generally concerns representation of the uncertainties of TRACG model parameters that affect the prediction of void fraction in the core and bypass. The core and bypass are distinguished from the regions of the vessel by their comparatively small hydraulic diameters. Two sets of TRACG comparisons with test data were used to define the bias and uncertainty of parameters influencing core and bypass void fraction for ATWS calculations. As described in the AOO application report [12], data from the FRIGG test facility [11], which form the basis for the GE design void correlation, are the most relevant data for pressures within or near the normal operating range. [[Proprietary Information Redacted]]

For LOCA and ATWS application, the database for specifying the void uncertainty was augmented by comparisons of TRACG predictions with a series of low-pressure void fraction tests performed by Toshiba [22], [23]. These tests were conducted with a 16-rod bundle at pressures of 0.50 and 1.00 MPa. A total of 15 tests were run over a range of bundle powers at two mass fluxes. A statistical summary of the deviations between the TRACG predictions and the Toshiba void fraction measurements is shown in Figure 5.1-8. TRACG predicted the Toshiba data with a negligible bias and a standard deviation of [[Proprietary Information Redacted]]. Figure 5.1-8 indicates that it is reasonable to assume that the void fraction deviations are normally distributed.

[[Proprietary Information Redacted]]

[[Proprietary Information Redacted]]

Figure 5.1-8. Void Fraction Deviations for Toshiba Tests

[[Proprietary Information Redacted]]

Figure 5.1-9. Sensitivity of TRACG Prediction of Toshiba Void Fraction to PIRT Multiplier on (C_o-1)

[[Proprietary Information Redacted]]

Figure 5.1-10. Sensitivity of TRACG Prediction of Toshiba Void Fraction to PIRT Multiplier on Entrainment Coefficient, η
[Proprietary Information Redacted]]

Figure 5.1-11. Lognormal Probability Distribution for PIRT22 and PIRT52

C2BX   Subcooled Void Fraction

The void fraction in the subcooled flow regime is quite insensitive to the magnitude of the heat transfer coefficients at the interface between the bubbles and the subcooled liquid, as long as a reasonable value is used. The void fraction is more sensitive to the liquid enthalpy at which net vapor generation occurs (h_{ld}), and to the distribution of the surface heat flux going into vapor generation versus liquid superheat at the wall ($q"_l$). The Saha-Zuber criterion is used for h_{ld} and the Rouhani-Bowring model is used to calculate the fraction of the wall heat flux to the liquid, $q"_l$ [14]. Of these, the void fraction is most affected by h_{ld} . Reference 24 shows that the scatter in the prediction of the subcooling at the net vapor generation point, h_f - h_{ld} , can be bounded by $\pm$ [[Proprietary Information Redacted]]. Comparisons to 8x8 bundle void fraction data show that the larger scatter in the void fraction for low qualities in the subcooled boiling region ([[Proprietary Information Redacted]] for the fully developed nucleate boiling region) is covered when a [[Proprietary Information Redacted]] perturbation is applied to the subcooling for the onset of net vapor generation. The mean error is also slightly larger for subcooled boiling ([[Proprietary Information Redacted]]). The statistical analysis of the comparison to the subcooled void fraction data is shown in Figure 5.1-12.

A [[Proprietary Information Redacted]] variation in the subcooling for onset of net vapor generation corresponds to an average of [[Proprietary Information Redacted]] and a maximum of [[Proprietary Information Redacted]] variation in the void fraction for the subcooled boiling region. Therefore a 1σ uncertainty of [[Proprietary Information Redacted]] is assigned for this model. The impact on the calculated void fraction at the FRIGG test conditions of a PIRT multiplier (PIRT23) value of [[Proprietary Information Redacted]] is seen in Figure 5.1-13.

[[Proprietary Information Redacted]]

Figure 5.1-12. FRIGG OF64 Void Fraction Data – Subcooled Boiling
[[Proprietary Information Redacted]]

Figure 5.1-13. Void Fraction Sensitivity to PIRT23

C3AX   Pellet Heat Distribution

The pellet power distribution is calculated by lattice physics codes and provided as an input to TRACG. Uncertainties in this parameter are reflected in the pellet temperature distribution, which is the parameter for which data are available. [[Proprietary Information Redacted]] Sensitivity studies show that the distribution calculated by lattice physics codes provides conservative results compared to a flat power distribution.

C3BX   Pellet Heat Transfer Parameters

The TRACG fuel rod model is based on the GESTR model [25]. The uncertainty in measured fuel centerline to coolant temperature differences is [[Proprietary Information Redacted]] and includes uncertainty in gap size and conductance, pellet conductivity and power distribution. The uncertainties in pellet power distribution, conductivity and gap conductance are lumped into a single uncertainty in the fuel conductivity, in qualifying the overall model against fuel temperature data. The dominant resistance is the pellet conductivity; an [[Proprietary Information Redacted]] variation in the pellet conductivity corresponds to the [[Proprietary Information Redacted]] observed uncertainty in the centerline to coolant difference, while the gap conductance needs to be varied by a factor of [[Proprietary Information Redacted]] to produce the same variation in the temperature difference as shown in Figure 5.1-14 and Figure 5.1-15. In these figures, PIRT27 is a multiplier on the fuel thermal conductivity and PIRT28 is the multiplier on the gap conductance. When the gap conductance is increased, the resistance over the gap becomes insignificant compared to the thermal resistance of the pellet, and it is not possible to vary the temperature difference to the 2σ level needed to produce a 95% probability estimate. Furthermore, normal distribution in the gap conductance would not produce a normal distribution in the center to fluid temperature difference due to the highly non-linear relationship between the gap conductance and the fuel center to fluid temperature difference.

[[Proprietary Information Redacted]]

[[Proprietary Information Redacted]]

Figure 5.1-14. Sensitivity of Fuel Center to Fluid Temperature Difference for 8x8 Fuel
[[Proprietary Information Redacted]]

Figure 5.1-15. Sensitivity of Fuel Center to Fluid Temperature Difference for 9x9 Fuel

C3CX   Gap Conductance

[[Proprietary Information Redacted]]

C3   Variable Gap Conductance

The uncertainty in C3 is covered under C3BX.

C4   Flashing in Core

The uncertainty in flashing in the core region is taken into account through the uncertainty in liquid-side interfacial heat transfer. The magnitude of the interfacial heat transfer at the bubble surface is varied through a lognormal probability distribution as described above under B1.

C8   Multiple Channel Effect

The flow distribution between parallel flow paths such as the fuel channels in the core is controlled by the hydraulic characteristics of the channels. The flow in each individual channel is controlled by the pressure drop components such as static head (given by the void fraction), friction and accelerational pressure drop. Therefore, the uncertainty in the flow in the individual channels and the parallel channel effects are covered by the uncertainty in the interfacial shear and the friction factors. The uncertainty in the interfacial shear is defined in Item C2AX and the uncertainty in friction factors is defined in Item C24.

In addition to the uncertainty in void fraction and friction, the channel pressure drop is dependent on the channel power level and axial distribution. The modeling of the core is derived from the code qualification studies in Reference 11. [[Proprietary Information Redacted]]

C10   Void Distribution, Axial and Between Channels

The uncertainty in the void fraction distribution is included through an uncertainty in the interfacial shear. The uncertainty in interfacial shear is defined in Item C2AX.

C11   Bundle – Bypass Leakage Flow

The channel leakage flow is based on full-scale measurements for conditions covering the range of expected reactor conditions [26]. [[Proprietary Information Redacted]]

C12   Natural Circulation Flow

Natural circulation is controlled by a balance between buoyancy and friction. Therefore, the uncertainty in this phenomenon is covered by the uncertainty in interfacial shear (which determines the void fractions) and the uncertainty in the friction factors and form losses. The uncertainty in interfacial shear is defined in Items C2AX, E2 and F1, and the uncertainty in frictional losses is defined in Items A11, C24 and I3.

C13   Dryout (Steady State and Transient Effects)

Dryout is calculated to occur when the critical power/quality is exceeded; rewet will occur if critical power/quality is no longer exceeded and the wall temperature is below the minimum film boiling temperature Tmin (C20). Critical power/quality is calculated with the GEXL boiling length correlation or either the modified Zuber or Biasi critical heat flux (CHF) correlations, depending on

the flow conditions. The manner in which these correlations are employed depends on the direction of the liquid and vapor flows. For cocurrent upflow, the GEXL correlation is used for critical power. For countercurrent flow and cocurrent downflow, CHF is calculated with either the modified Zuber or Biasi correlation, depending on mass flux. In practical terms, the Biasi correlation is used in very limited circumstances involving high flow conditions.

The GEXL correlation was derived from full-scale ATLAS data. The correlation typically has a small bias and a standard deviation between 3 and 4% depending on fuel type. [[Proprietary Information Redacted]]The uncertainty is applied with a normal distribution.

An uncertainty in the modified Zuber correlation was derived by comparisons with the CHF data of Walkush [28]. Walkush obtained CHF data for flow through a vertical annulus with a heated inner ring. The measurements included tests with countercurrent flow and cocurrent upflow and downflow. The CHF data were correlated vs. exit void fraction for void fractions ranging from 10 to 70%. The distribution of the fractional deviations between the modified Zuber correlation and the Walkush measurements is shown in Figure 5.1-16. The deviations are well represented by a normal distribution with a conservative bias of [[Proprietary Information Redacted]]

[[Proprietary Information Redacted]]

Figure 5.1-16. Fractional Error in Modified Zuber Critical Heat Flux Correlation

Reference 14 presents information from a number of sources on comparisons between the Biasi CHF correlation and experimental data. The RMS error in the correlation with respect to the database from which it was originally derived was reported to be 7.3% [29]. Comparison of the Biasi correlation with 1928 data points from a Harwell round-tube data bank [30] gave a bias of −8% and a standard deviation of 17%. Comparison of the correlation with experimental points from a number of other data banks [31] showed that 73% and 99% of the data were within 30% of the correlation for constant dryout quality and constant inlet subcooling, respectively. On the basis of this collection of data comparisons, a [[Proprietary Information Redacted]] was specified for the Biasi correlation.

C15   Film Boiling (Dispersed Flow)

Heat transfer for film boiling under dispersed flow conditions is calculated in TRACG with the Sun-Gonzalez-Tien heat transfer coefficient. The uncertainty in the Sun-Gonzalez-Tien heat transfer coefficient is assumed to be the same as the uncertainty in the Dittus-Boelter heat transfer coefficient for steam cooling conditions (C17). A second parameter influencing heat transfer under dispersed flow conditions is vapor side interfacial heat transfer. As in the case of liquid-side interfacial heat transfer (A1), TRACG uses the Lee-Ryley correlation in conjunction with a bubble diameter based on a critical Weber number to calculate vapor-side interfacial heat transfer in the dispersed flow regime [14]. [[Proprietary Information Redacted]]

C17   Steam Cooling (H)

TRACG calculates heat transfer to superheated steam with the Dittus-Boelter heat transfer coefficient [14]. An extensive investigation of heat transfer to superheated steam in a rod bundle is presented in Reference 33. Reference 33 describes a series of steady-state tests over a pressure range from 13.1 to 40.7 bar and a mass flux range from 33.9 to 169.6 kg/m^2-s. The tests were conducted in an interior-peaked rod bundle with an outlet-peaked axial heat flux profile. Measured rod temperatures were compared with predictions based on several heat transfer coefficients including Dittus-Boelter. Two approaches were used to calculate the local steam temperature for the predictions - a bundle average approach and an extended rod-centered subchannel approach. The bundle average approach resulted in a non-conservative bias of about [[Proprietary Information Redacted]] in the predicted wall temperatures. The extended rod-centered subchannel approach resulted in a conservative bias of slightly over [[Proprietary Information Redacted]]. The rms error in the predictions was [[Proprietary Information Redacted]] for the bundle average approach and [[Proprietary Information Redacted]] for the extended rod-centered subchannel approach. Combining the rms error with the mean bias gives a standard deviation of about [[Proprietary Information Redacted]] for both approaches. These results are summarized in the "Wall Temperature" columns of Figure 5.1-17.

Table 5.1-1. Error Measures for Wall Temperature [33]and Dittus-Boelter Heat Transfer Coefficient (Estimated)

[[Proprietary Information Redacted]]

The error on which the statistical evaluation in Reference 33 is based was defined as

$$Error(T) = \frac{T_{w,m} - T_{w,p}}{T_{w,m}}$$

where

    $T_{w,m}$ = measured wall temperature

    $T_{w,p}$ = predicted wall temperature

For purposes of TRACG analysis, our interest is in the corresponding error in the heat transfer coefficient, defined as

$$Error(h) = \frac{h_p - h_m}{h_p}$$

It is easily shown that

$$Error(h) = \frac{Error(T)}{1 - \frac{T_s}{T_{w,m}}} \quad \text{where } T_s = \text{steam temperature.}$$

It is obvious from this expression that the fractional error in the predicted heat transfer coefficient can be several times as large as that in the predicted wall temperature.

The data described in Reference 33 include 1935 measurement points. Of these, 60 points from four runs are shown graphically in the report along with the steam temperature calculated by both the bundle average and extended rod-centered subchannel approaches. On the basis of these 60 points, it was determined that [[Proprietary Information Redacted]]

The average values of the multipliers, determined on the basis of the 60 points for which the data are available, were used to estimate the mean bias and standard deviation for the Dittus-Boelter heat transfer coefficient as shown in the "Dittus-Boelter HTC" columns of Table 5.1-1

[[Proprietary Information Redacted]]

[[Proprietary Information Redacted]]

Figure 5.1-17. Fractional Error in Wall Temperature Calculated with the Dittus-Boelter Heat Transfer Coefficient

C19X   Tmin (Minimum Stable Film Boiling Temperature)

TRACG calculates the minimum film boiling temperature as the maximum of the homogeneous nucleation temperature and the Iloeje correlation [14]. For the Iloeje correlation, the estimated error in $T_{min} - T_{sat}$ for conditions near those of the database is 10%. For conditions significantly outside the mass flux and quality range of the data, 20% is the recommended uncertainty [14]. [[Proprietary Information Redacted]]

C24   Core Pressure Drop

The core pressure drop is composed of static head given by the void fraction, accelerational pressure drop and friction. The uncertainty in the core pressure drop is therefore covered by the uncertainty in the interfacial shear and friction. The uncertainty in interfacial shear is defined in Item C2AX.

TRACG uses the GE design correlation for the wall friction, [[Proprietary Information Redacted]] is based on extensive comparisons to rod bundle pressure drop data [14] from BWR bundles. For single-phase flow in smooth pipes TRACG predicts the pressure drop with an accuracy of [[Proprietary Information Redacted]] For two-phase flow, the majority of the comparisons with the [[Proprietary Information Redacted]] correlation have been made for rod bundle data. Data for GE14 10x10 fuel shows a [[Proprietary Information Redacted]] Based on this data, it is judged that [[Proprietary Information Redacted]] is adequate for all other applications. The components of the flow losses in the fuel bundle and the uncertainty associated with each component are discussed in the following paragraphs.

The side entry orifice and lower tie plate frictional pressure drop is based on full-scale measurements for conditions covering typical reactor operating conditions. The inlet orifice is a sharp-edged orifice with a well-defined flow coefficient. The inlet region upstream of the lower tie plate has turning losses and a flow expansion at the inlet. The lower tie plate accounts for approximately one third of the total pressure drop. Reference 14 shows that the typical scatter in the loss coefficient for the lower tie plate is of the order of [[Proprietary Information Redacted]] Data from GE's single-phase pressure drop test facility show that the uncertainty for the combined pressure drop for the side entry orifice and the lower tie plate pressure drop is approximately [[Proprietary Information Redacted]], when the entire uncertainty is assigned to the lower tie plate [12].

[[Proprietary Information Redacted]]

The spacer frictional pressure drop is based on full-scale measurements for conditions covering the range of expected reactor conditions. For 9x9 and 10x10 fuel spacers the uncertainty in the pressure drop for the spacers is determined from full-scale ATLAS data and varies from [[Proprietary Information Redacted]], depending on bundle type [12]. The average uncertainty for all fuel designs is of the order of [[Proprietary Information Redacted]] [12]

The upper tie plate frictional pressure drop is based on full-scale measurements for conditions covering the range of expected reactor conditions. For 9x9 and 10x10 fuel upper tie plates, the uncertainty in the pressure drop is [[Proprietary Information Redacted]] [12].

$$^{\{3\}}]]$$

Qualification of TRACG against full-scale bundle pressure drop data from the ATLAS facility for an 8x8 bundle with ferrule spacers [5.5] has shown that TRACG predicts the bundle pressure drop with a bias of [[Proprietary Information Redacted]] and a standard deviation of [[Proprietary Information Redacted]]. These comparisons for total pressure drop are consistent with the above uncertainties for the side entry orifice, lower tie plate, spacers and upper tie plate.

Based on the preceding discussion, the following approach will be adopted.

[[Proprietary Information Redacted]].

E2 Downcomer Void Profile / Two-Phase Level

The downcomer void fraction is determined by the interfacial drag coefficient, C_I. An appropriate uncertainty range for C_I was obtained for large hydraulic diameter regions as discussed below under F1. The downcomer two-phase level is an initial condition depending on the plant operating state. The uncertainty in this parameter is discussed in Section 6.

E7 Feedwater Sparger Uncovery/ Condensation

Condensation in the downcomer is controlled by liquid-side interfacial heat transfer, which is addressed in the same manner as described under B1.

F1 Chimney Void Distribution/two-Phase Level

The chimney void distribution is controlled by the interfacial drag coefficient, C_I. An appropriate uncertainty range for C_I was obtained on the basis of TRACG predictions of void fraction data from separate-effects tests by [[Proprietary Information Redacted]]. These data are characterized by their applicability to the prediction of void fraction in regions with relatively large hydraulic diameter. Accordingly, they will be used as the basis for defining the uncertainty in interfacial drag in all regions of the reactor except the core and bypass. A statistical summary of the comparisons of TRACG predictions with measurements from these four data sets, combined as a single set of deviations, is shown in Figure 5.1-18. [[Proprietary Information Redacted]].

[[Proprietary Information Redacted]]. The results are shown in Figure 5.1-19 [[Proprietary Information Redacted]].

[[Proprietary Information Redacted]]

Figure 5.1-18. Void Fraction Deviations for Tests Applicable to Regions with Large Hydraulic Diameter

[[Proprietary Information Redacted]]

Figure 5.1-19. Sensitivity of TRACG Prediction of Average Void Fraction in EBWR Test Facility to PIRT Multiplier on Interfacial Drag Coefficient
[[Proprietary Information Redacted]]

Figure 5.1-20. Probability Distribution for Multiplier on Interfacial Drag Coefficient

[[Proprietary Information Redacted]].

I1   Separator Carryunder

Separator carryunder affects the core inlet subcooling. Carryunder is calculated by the TRACG separator model. Typical values of carryunder at normal operation are of the order of [[Proprietary Information Redacted]]. An uncertainty of [[Proprietary Information Redacted]].(absolute) bounds the differences between TRACG and separator data and will be used as an estimate of the 1σ uncertainty in the model.

I2   Separator L/A

The separator inertia (L/A) has a small effect in rapid pressurization events. Reduced inertia increases the severity of the calculated transient. The spiraling liquid film along the separator barrel primarily determines the separator inertia. A 25% variation is representative of the 1σ uncertainty in the separator inertia [12].

I3   Separator Pressure Drop

The loss correlations for the separator pressure drop in TRACG are best fit to two and three stage separator pressure drop data [11]. 95% of the data falls within [[Proprietary Information Redacted]] of the correlation, which has been implemented into TRACG. 95% corresponds to the 2σ level and therefore [[Proprietary Information Redacted]] is a good approximation for the 1σ uncertainty in separator pressure drop.

L1   Critical Flow through SRV

The uncertainty in the critical flow model has been assessed for TRACG [11], and a zero bias and a 1σ uncertainty of [[Proprietary Information Redacted]] was determined to be appropriate. However, for ATWS application the nameplate capacity of the SRVs is specified and used as a limiting value. This value is not varied in the sensitivity studies.

L2X   Acoustic Effects in Steamline

Sudden closure of the turbine stop valves or control valves results in the propagation of a pressure pulse at sonic speed from the valve to the steam dome. (This effect is less severe for the slower closing of the MSIVs). The timing and arrival of the pressure pulse has a significant effect on the severity of the transient. The uncertainty in the sonic propagation speed comes primarily from the carryover of liquid droplets into the steamlines. TRACG uses a bounding assumption of perfect separation of droplets from the steam in the dryer, and therefore evaluates the steam line response

with dry steam. This conservatively maximizes the velocity of sound in the steam line and produces a bounding power peak for the pressurization event.

Q2   Isolation Condenser Capacity

Full-scale tests were performed of an Isolation Condenser (IC) module in the PANTHERS test facility. Comparisons with TRACG results showed a negative bias of [[Proprietary Information Redacted]] and a 1σ uncertainty of [[Proprietary Information Redacted]] in the total heat removal rate [15].

Q5   Isolation Condenser Secondary Side Heat Transfer

The uncertainties in the secondary side heat transfer are included in the data for the overall condenser heat removal (Q2) above.

Table 5.1-2. Bias and Uncertainty for High Ranked ATWS Model Parameters

[[Proprietary Information Redacted]]

5.2 Effects of Nodalization

The nodalization strategy for the various reactor components was developed from the qualification of TRACG against test data for these components. The same consistent nodalization strategy was then applied for full-scale plant calculations. The adequacy of the nodalization has been demonstrated and supported by sensitivity studies. Standard nodalization for modeling of BWR reactor vessels and other components have been presented in the *TRACG Qualification Report* [11]

The nodalization for ATWS is the same as that used for ESBWR stability [19] [[Proprietary Information Redacted]].

5.2.1 Vessel Nodalization for ESBWR ATWS Analysis

Figure 8.1-1 shows the axial and radial nodalization of the ESBWR vessel. The axial levels and radial rings are the same as used previously for stability analysis for the ESBWR. [[Proprietary Information Redacted]]

5.2.2 Channel Grouping for ATWS Applications

Individual fuel bundles in the core may be modeled in TRACG as individual channels or may be grouped together into a single TRACG channel component. Because of current code limitations within TRACG on the number of components allowed, it is not possible to model every fuel bundle as a single TRACG channel. Consequently, it is necessary to group or combine individual fuel bundles into thermal hydraulic groups. [[Proprietary Information Redacted]]

The channels are grouped based on (a) hydraulic considerations to separate hydrodynamic characteristics and (b) neutron kinetics considerations to separate dynamic power sensitivity characteristics.

The channel grouping accounts for additional TRACG capability in the areas of limiting channel response, peripheral channel grouping, and vessel modeling detail. [[Proprietary Information Redacted]]

Figure 8.1-3 shows the typical grouping of channel components for ATWS analysis. [[Proprietary Information Redacted]].

5.3 Effects of Scale

Effects of scale have been specifically addressed as part of the model development as well as the qualification. In the TRACG model description report [14], the ranges of applicability of the basic models and correlations are stated and shown to cover the scale and operating range of BWRs [Table 6.0-1 of Reference 14]. This is a *necessary* condition for the validity of TRACG calculations for the full-scale BWR.

The qualification of TRACG [11] covers separate-effects tests, full and reduced scale component performance tests, scaled integral system effects tests, and full-scale BWR plant tests. Accurate

predictions of data at various scales (up to a sufficiently large scale) constitute a *sufficient* condition for the validity of TRACG calculations for full-scale plants. In general, the qualification results show that both data from scaled test facilities as well as full-scale plant data are well predicted, and that there is no apparent effect of scale in the TRACG calculations.

The conclusion that there is no effect of scale in the TRACG calculations is substantiated in this section.

5.3.1   Full Scale Test Coverage

Table 3.2 shows the coverage of the Medium and High ranked PIRTs for ATWS by test data. A number of ESBWR components have been tested at full scale. [[Proprietary Information Redacted]].

5.3.2   Operating Plant Data

Tests performed at BWR plants validate a number of phenomena that are highly ranked for ATWS. [[Proprietary Information Redacted]].

In summary, TRACG has been validated over a range of test data and no additional uncertainty is needed to account for scale-up effects.

5.4   Sensitivity Analysis

Sensitivity studies have been performed, varying each highly ranked model parameter from -1σ to $+1\sigma$. These results are shown in Section 8. These studies serve to identify the parameters that have the largest impact on the calculated safety parameters (vessel pressure, PCT, containment pressure and suppression pool temperature).

6.0 APPLICATION UNCERTAINTIES AND BIASES

6.1 Input

Specific inputs for each transient event are specified via internal procedures, which are the primary means used by GE to control application of engineering computer programs. The specific code input will be developed in connection with the Application Licensing Topical Report (LTR), the NRC SER and the development of the application specific procedure. This section will be limited to a more general discussion of how input is treated with respect to quantifying the impact on the calculated results. As such, it serves as a basis for the development of the application specific procedures.

Code inputs can be divided into four broad categories: (1) geometry inputs; (2) model selection inputs; (3) initial condition inputs; and (4) plant parameters. For each type of input, it is necessary to specify the value of the input. A discussion of categories (1) and (2) is contained in Section 6.1 of Reference 1. Since initial conditions and plant parameters will be handled slightly differently for ATWS analyses than for AOOs, Section 6.2 and Section 6.3 provide the basis for ATWS initial conditions and plant parameters.

6.2 Initial Conditions

As described in Section 6.2 of Reference 1 *initial conditions* are those conditions that define a steady-state operating condition. Initial conditions may vary due to the allowable operating range or due to uncertainty in the measurement at a given operating condition. The key plant initial conditions and associated uncertainties are given in Table 8.2-1.

Due to the extremely low probability of the occurrence of an ATWS, the NRC Staff has accepted nominal initial conditions for ATWS analysis. However, as previously mentioned, defining a nominal initial condition is not always straightforward. Consequently, the transients will be initiated from the limiting point(s) in the allowed operating domain. Specifically, the impact of a particular initial condition on the results is characterized in the following manner:

- The results are sensitive to the initial condition and a basis for the limiting initial condition cannot be established. Future plant analyses will consider the full allowable range of the initial condition.

- The results are sensitive to the initial condition and a basis for the limiting initial condition can be established. Future plant analyses will consider the parameter to be at its limiting initial condition.

- The results are not sensitive to the initial condition and a nominal initial condition will be assumed for the parameter.

Consistent with past ATWS licensing analyses, initial conditions will not be adjusted to account for instrumentation or simulation uncertainties. As demonstrated in Section 8 (see Table 8.2-2), the PCT

is sensitive to uncertainties in power, feedwater enthalpy, pressure setpoint and core exposure. The peak power is sensitive only to the core exposure. Other parameters are not significantly affected.

6.3 Plant Parameters

A *plant parameter* is defined as a plant-specific quantity such as a protection system setpoint, valve capacity or stroke time, or a scram characteristic, etc. *Plant parameters* influence the characteristics of the transient response and have essentially no impact on steady-state operation, whereas *initial conditions* are what define a steady-state operating condition.

Due to the extremely low probability of the occurrence of an ATWS, the NRC Staff has accepted nominal plant parameters for ATWS analysis. AOO transient analyses require [12] application of conservative *analytic limits* for plant parameters. The value of the analytical limit (AL) can be typically related to the plant technical specification (Tech Specs) as discussed in Section 6.3 of Reference 1. Application of an analytic limit for ATWS overpressure is simpler to apply and less difficult to defend than nominal plant parameters. Analytical limits will be applied for the ESBWR ATWS analyses unless it is determined that the sensitivity to a plant parameter is not significant. Table 8.2-4 presents the plant parameters that were examined as part of this study.

GE procedures for Customer Technical Requirements (CTRs) require that both GE and the Licensee agree to design input. All critical ATWS plant parameters will be reviewed in this manner.

7.0 COMBINATION OF UNCERTAINTIES

7.1 Approaches for Combining Uncertainties

In order to determine the total uncertainty in predictions with a computer code, it is necessary to combine the uncertainties due to model uncertainties (CSAU Step 9), scaling uncertainties (CSAU step 10), and plant condition or state uncertainties (CSAU Step 11). Various methods have been used to combine the effects of uncertainties in safety analysis. Section 7.3 of Reference 12 summarizes different methods for combining uncertainties. The approaches described are within the framework of the CSAU methodology, since the CSAU methodology does not prescribe the approach to use. Table 7-1 gives a summary description of different methods of combining uncertainties. Table 7-2 summaries the pros and cons of each approach.

Table 7-1 Methods for Combining Uncertainty

Method	Description
Propagation of Errors	Uncertainties in the calculated safety parameters to individual phenomena are evaluated from single perturbations and the overall uncertainty is determined as the square root of the sum of the squares of the individual uncertainties.
Response Surface Technique	Response surface for the safety parameter is generated from parameter perturbations. Statistical upper bound is determined from the Monte Carlo method using a response surface.
Order Statistics Method - Single Bounding Value (GRS Method)	Monte Carlo method using random perturbations of all important parameters. Sample size defined to yield desired statistical confidence. Statistical upper bound is determined from most limiting perturbation (for first order statistics).
[[Proprietary Information Redacted	]]

Table 7-2 Comparisons of Methods for Combining Uncertainties

Method for Combining Uncertainties	Advantages	Disadvantages
Propagation of Errors	Relatively small number computer runs, when the number of input variables is small. The number of cases is linearly related to the number of input parameter uncertainties considered.	Approximate because it involves linearization. Necessary either to demonstrate independence of effects of individual uncertainties on responses, or else must include covariances explicitly.
Response Surface	Very precise statistical characterization of results with a large number of Monte Carlo Trials using response surface. Different distributions can be specified for each input uncertainty. Independence of the effect of individual input parameters on response is not necessary.	Number of computer runs depends on the response surface model and increases exponentially with the number of input parameter uncertainties considered. Interactions between input parameters have to be established and considered in the development of the response surface.
Order Statistics (GRS)	The number of random trials is independent of the number of input parameters considered. The method requires no assumption about the PDF of the output parameter. It is not necessary to perform separate calculations to determine the sensitivity of the response to individual input parameters. It is not necessary to make assumptions about the effect on the output of interactions of input parameters.	Since the tolerance limits are based on order statistics, they will vary from one set of TRACG trials to another, and these differences may be substantial, especially for small sets of TRACG trials, and particularly if the tolerance bound is the sample extreme.
[[Proprietary Information Redacted		]]

7.2 Recommended Approach for Combining Uncertainties

[[Proprietary Information Redacted]]

7.3 Statistical Analysis for Qualification Events

Section 7.6 of Reference 12 provides a statistical analysis of selected AOO events. Since there is no ATWS transient event to compare to, these events provide the best possible evaluation of TRACG's

accuracy. They provide a general confirmation that the code uncertainty determined by varying PIRT parameters is consistent with the event measurements.

8.0 DEMONSTRATION ANALYSIS

The TRACG performance is demonstrated on the MSIVC, LCV, and LFWH scenarios specified in Section 2.7. This demonstration includes:

1. A TRACG baseline analysis for the three category 1 scenarios using an equilibrium core designed for the ESBWR,

2. A demonstration of the sensitivity of the transient to initial conditions and plant parameters for the limiting scenario of MSIVC, and

3. A demonstration of the sensitivity of the transient to the individual model uncertainties using the limiting scenario of MSIVC.

The analyses provided in this section form the bases for future application of TRACG for the ESBWR. The baseline analysis (Section 8.1) is a demonstration of the process. The initial conditions (Section 8.2.1) and plant parameters (Section 8.2.2) analyses are performed to determine the sensitivity to the critical parameters. Section 8.2.3 contains details of analyses performed to demonstrate core stability during an ATWS event. Section 8.3 presents the analyses performed to quantify the sensitivity of the critical parameters to individual model uncertainties.

8.1 Baseline Analysis

The ESBWR plant has 1132 bundles and a rated thermal power of 4500 MWth. The vessel modeling is illustrated in Figure 8.1-1. The plant has an equilibrium core of GE14 10x10 fuel. Figure 8.1-2 also shows the average bundle power in the core sectors utilized in the model for azimuthal nodalization. The bundles in Ring 3 are grouped into two groups, with the bundles with inlet orificing corresponding to the peripheral region having a much lower average power level. Figure 8.1-3 illustrates the TRACG core map showing the thermal hydraulic channel groups. The number of channels in each thermal hydraulic group and the peaking factors for each group are shown in Table 8.1-1. Channel groups were created based on core position, chimney position, orifice geometry, and peaking factor. [[Proprietary Information Redacted]]

The model used for the baseline analysis has a simple model of the S/RV discharge line and the suppression pool (see Figure 8.1-4). The pool cooling system is modeled using the TRACG control system.

The SLCS system in the ESBWR consists of two accumulators, each pressurized to 17.2 MPa, which adiabatically expand upon opening the valves to inject the hot shutdown volume of 10.8 m³ (5.4 m³ from each accumulator) at an approximate vessel pressure of 8.6 MPa.

The SLCS is modeled using the TRACG control system and a flow velocity profile versus time for the accumulators. The average velocity at the flow nozzles that inject the solution into the bypass region is 30.5 m/s during the first half of the injection of the volume stipulated to achieve hot shutdown. Based on the velocity versus time profile, the total volume of 10.8 m³ is injected at high pressure into the bypass in about 9 minutes. A delay time of 2s for the SLCS valve opening and a further delay of 3s for the solution to reach the nozzle after initiation are assumed. This is in addition

to the 180s delay for SLCS initiation amounting to a total delay of 189 seconds (for the MSIVC case) after the start of the transient.

[[Proprietary Information Redacted]]

Figure 8.1-1. TRACG ESBWR Vessel R-Z Modeling

[[Proprietary Information Redacted]]

Figure 8.1-2. TRACG Core Map with Sector Average Bundle Power

[[Proprietary Information Redacted]]

Figure 8.1-3. TRACG Channel Grouping for ESBWR Core

[[Proprietary Information Redacted]]

Figure 8.1-4. SR/V Discharge Line and Suppression Pool Nodalization

Table 8.1-1. TRACG Channel Grouping (MOC)
[[Proprietary Information Redacted]]

The baseline model also has conservatisms included in it to bound model phenomena or certain plant component specifications. [[Proprietary Information Redacted]]

8.1.1 MSIV Closure ATWS (MSIVC) Baseline Analysis

The MSIV stroke time for these analyses is set at the minimum value of 3s. ESBWR includes an automated feedwater runback on ATWS signal, to reduce core power. This is modeled through the feedwater level control system. To simulate the FW runback, and EPG actions, the vessel level setpoint is dropped to 1.524m (5') above TAF over a period of 15s and maintained at this minimum level through the event. Analyses were performed to ensure that refilling the vessel did not lead to recriticality. The suppression pool cooling model is activated at the set point of 322K. A hot rod model is included for the four hot channels. In addition, a bundle power peaking is applied to one of the hot channels to operate at a CPR of 1.2; this is conservatively lower than the present OLMCPR of 1.3 and provides margin for future reduction in the OLMCPR. This adds a further measure of conservatism to the model from a standpoint of the radial peaking. Table 8.1-2 presents the initial conditions, Table 8.1-3 presents the equipment performance characteristics as modeled in the baseline analysis, and Table 8.1-4 presents a summary of main events in the transient scenario.

Table 8.1-2. ATWS Initial Operating Conditions

Parameters	Value
Dome Pressure, MPa (psia)	7.17 (1040)
Power, MW	4500
Steam/Feed Flow, kg/sec (Mlbm/hr)	2433 (19.31)
Feedwater Temperature, °C (°F)	215.6 (420)
Initial Suppression Pool Temperature, °C (°F)	43.3 (110)

Table 8.1-3. ATWS Equipment Performance Characteristics

Parameters	Value
Nominal MSIV Closure Time, sec	3.0
Safety/Relief Valve (S/RV) System Capacity, % of Rated Steam Flow / No. of Valves	≥89.5 / 18
S/RV Setpoint Range, MPaG (psig)	8.618 to 8.756 (1250-

Parameters	Value
	1270)
S/RV Opening Time, sec	<0.2
ATWS Dome Pressure Sensor Time Constant, sec	0.5
ATWS Logic Time Delay, sec	≤1
Pool Cooling Capacity, KW/C	430.6
Temperature For Automatic Pool Cooling, °C (°F)	48.9 (120)

The steam line isolation causes a rapid increase in reactor vessel pressure (see Figure 8.1-8), which results in core void reduction (see Figure 8.1-12). Consequently, power increases (see Figures 8.1-5 and 8.1-12) with positive void reactivity insertion (see Figure 8.1-10). For ATWS simulation purposes, the expected MSIV position and high flux scrams do not occur. The power excursion is initially mitigated by void production from the increased core heat flux, as well as negative Doppler reactivity from increasing fuel temperature. High-pressure signals and APRM not downscale will initiate feedwater runback to minimum flow (see Figures 8.1-5 and 8.1-6). Feedwater runback results in dropping the water level (see Figure 8.1-7), stopping the recirculation of liquid through the steam separators, reducing channel flow (see Figure 8.1-9), increasing core void fraction and reducing power level. The isolation condensers (see Figure 8.1-6) will also activate at this point. At about the same time, the Safety/Relief Valves (S/RVs) open (see Figure 8.1-6), reducing the rate of pressure increase. As core flow continues to decrease, core voiding increases, causing the power to decrease in parallel. The pressure peaks and finally, as the steam production decreases to the point at which the S/RV capacity is sufficient to relieve all of the steam generation, and the pressure begins to fall (see Figure 8.1-8). The peak-clad temperature also occurs shortly after the pressure peaks. The pressure drops to about 8.5 MPa (around 120s) and remains at approximately this value until the SLCS initiation. The pressure begins to drop shortly after the boron begins to shut down the reactor.

Table 8.1-4. Sequence of Events for MSIVC

Time (s)	Event
0	MSIV Closure starts
0.3	Feedwater runback initiated
2	IC initiation
4	ATWS trip set at high pressure
5	SRVs open

19	Suppression pool cooling starts
25	Feedwater runback complete
42	Level drops below L2 set point
52	HPCRD flow starts
189	SLCS injection starts
312	Peak Pool Temperature
384	Hot shutdown achieved
710	High pressure design volume of borated solution injected into bypass

At approximately 188.5s (trip time of 3.5s+ 180s delay+ 5s delay for valve opening and initial flow at nozzle), the SLCS flow is activated (see Figure 8.1-10) and the borated solution starts to flow into the bypass. With the external circulation loop cut off by the low water level (see Figure 8.1-7), flow to the fuel channels from the vessel lower plenum will match what is required to makeup for steam generation in the core. The total channel mass flow will be higher than this, due to liquid entering from the core bypass through the Lower Tie Plate (LTP) holes. The LTP flow direction is reversed from normal operation. Liquid exiting the top of channels recirculates down the bypass, and re-enters the LTP holes. Because the flow in the bypass is downward under these conditions, the diluted plume of boron will move with the bulk bypass flow. Boron will enter the LTP holes and flow up the channel. [[Proprietary Information Redacted]] As boron is transported to the center of the core, the power level drops due to the large negative reactivity insertion (see Figure 8.1-10) and reaches decay heat levels after 159s from the time of injection (power is within half a percent of the decay heat). The S/RV discharge into the suppression pool stops at about 450s into the transient and the pool temperature peaks at [[Proprietary Information Redacted]]. This is well below the HCTL limit for the pool at the corresponding dome pressure (see Figure 8.1-11).

Table 8.1-5 summarizes the key results from the baseline analysis of the MSIVC event.

Table 8.1-5. Key Results from MSIVC

Parameter	Value	Time
Maximum Neutron Flux, %	228	3s
Maximum Vessel Bottom Pressure, MPaG (psig)	9.76 (1415)	29s
Maximum Bulk Suppression Pool Temperature, °C (°F)	78.0 (172.5)	312s
Associated Containment Pressure, MPaG (psig)	0.193(27.92)	312s
Peak Cladding Temperature, °C (°F)	915.5(1679.8)	24s
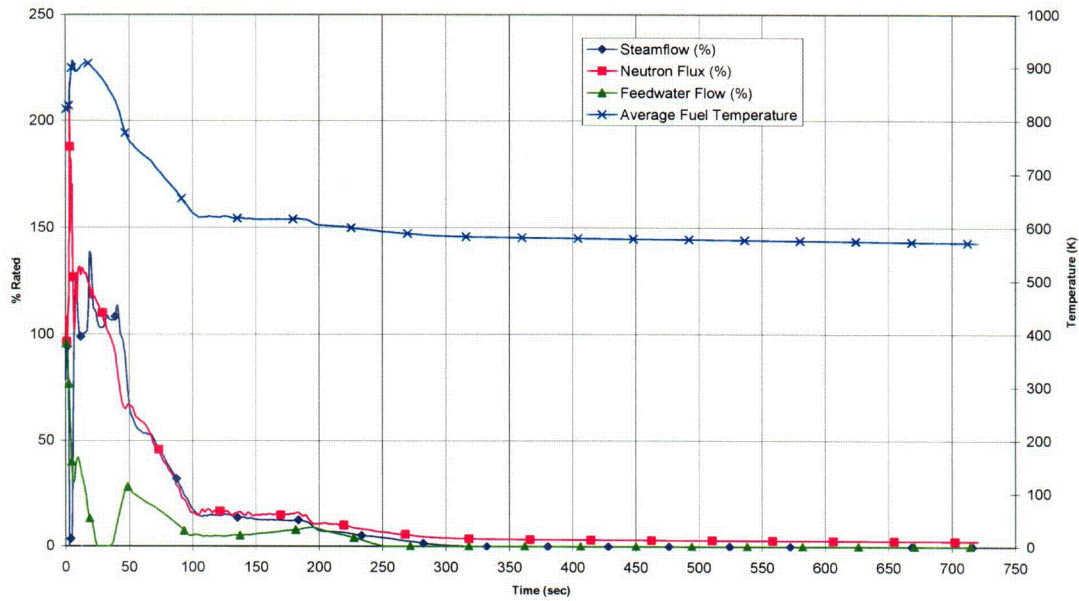
Figure 8.1-5. MSIVC Neutron Flux and Core Flow
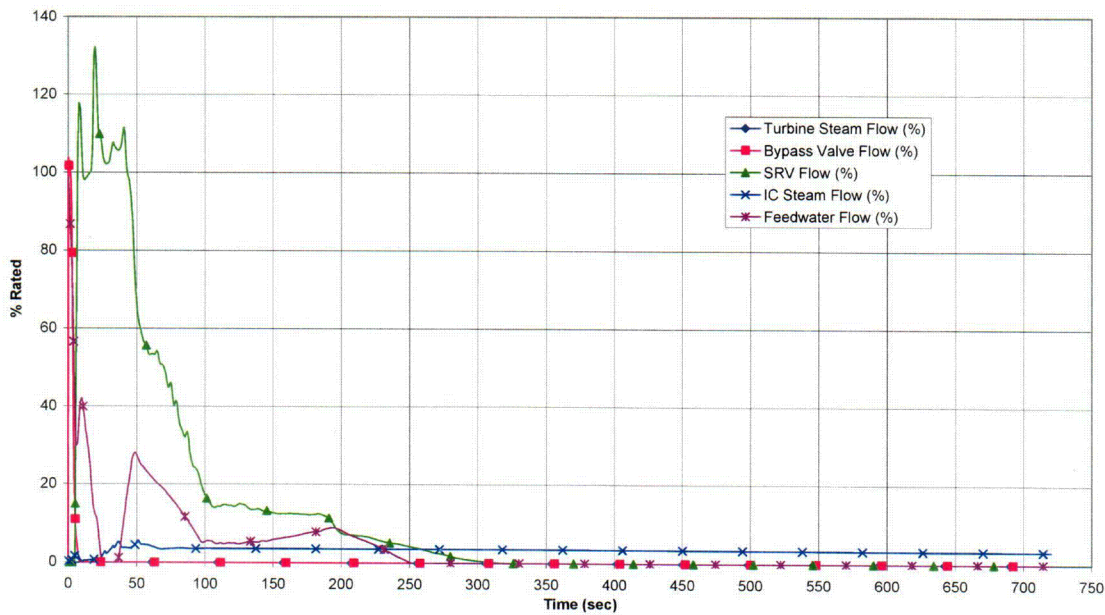
Figure 8.1-6. MSIVC Steam and Feedwater Flow

C03

Demonstration Analysis

DISK403:[SS.ESBWR.ATWS.MSIV.LTR]
Proc.ID: 2020CE60
30-AUG-2005 23:00:43.27

ATWS-MSIV-EOC-BOUND-SEP05_DCD.CDR;1

Figure 8.1-7. MSIVC Water Levels

DISK403:[SS.ESBWR.ATWS.MSIV.LTR]
Proc.ID: 2020CE60
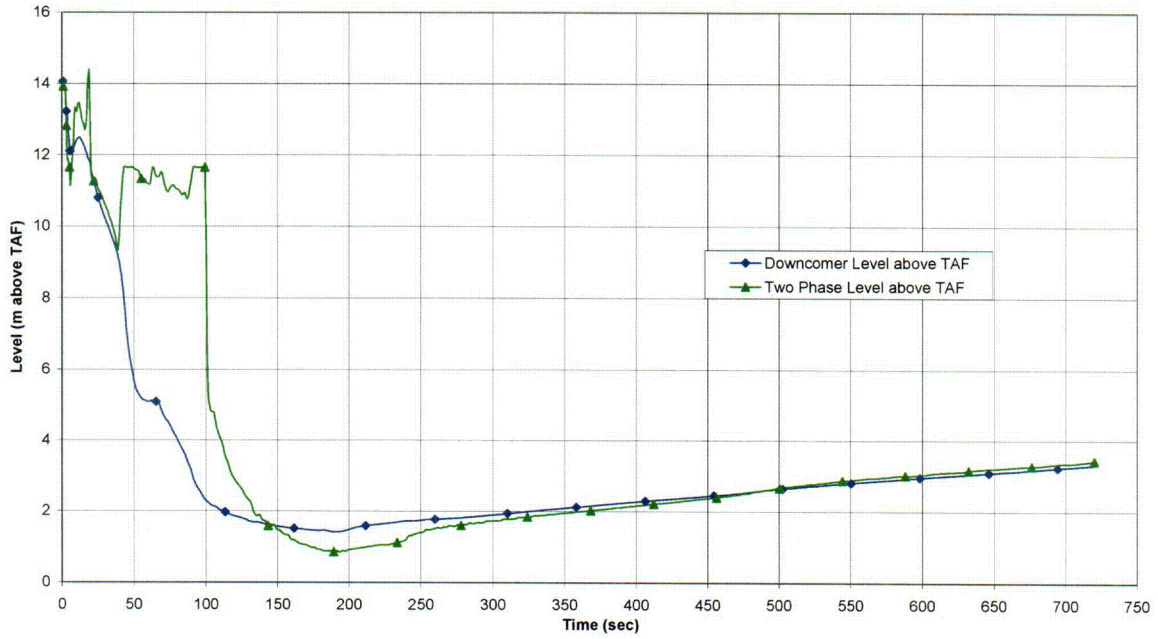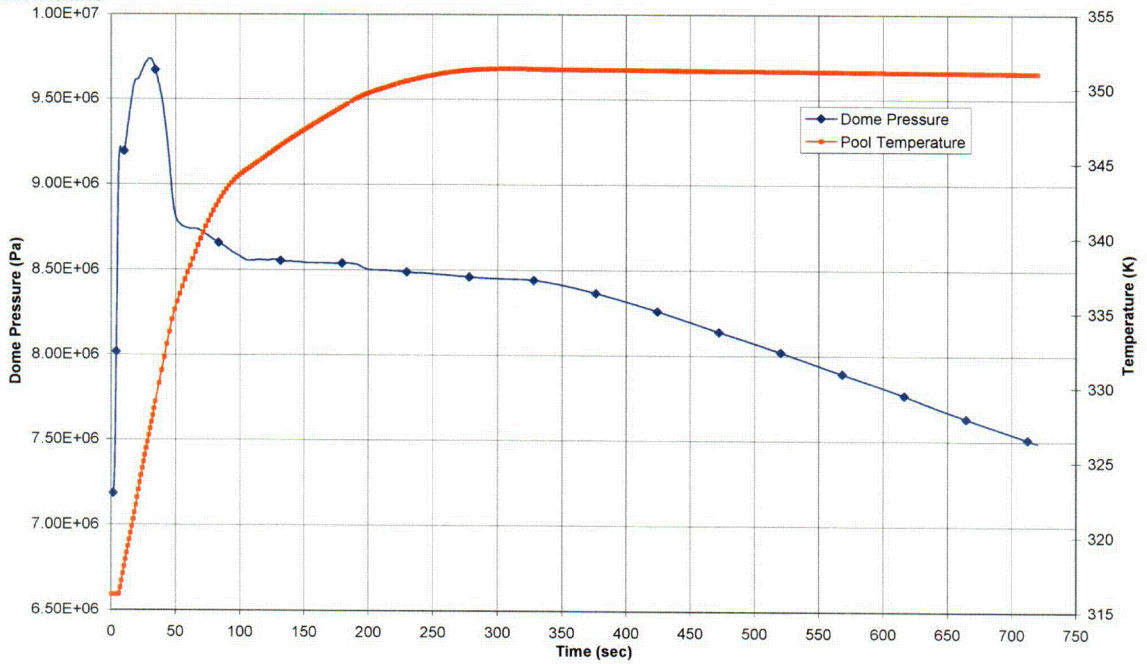30-AUG-2005 23:00:43.27

ATWS-MSIV-EOC-BOUND-SEP05_DCD.CDR;1

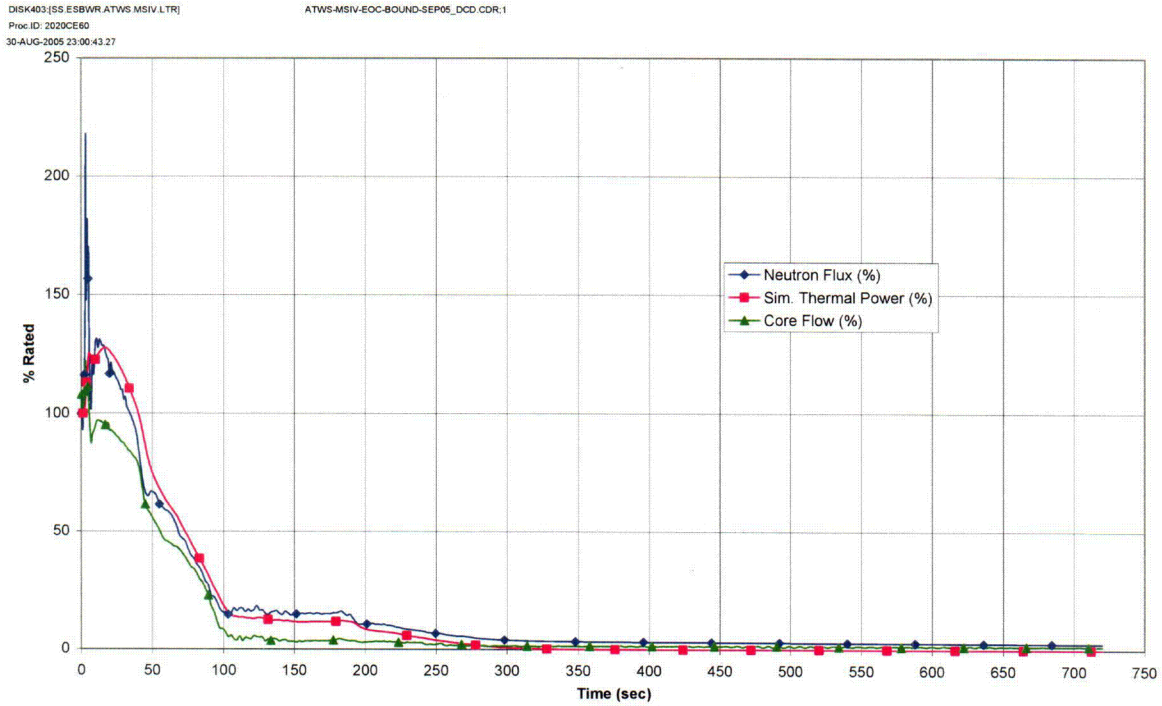**Figure 8.1-8. MSIVC Dome Pressure and Pool Temperature**

Demonstration Analysis

Figure 8.1-9. MSIVC Neutron Flux and Core Flow

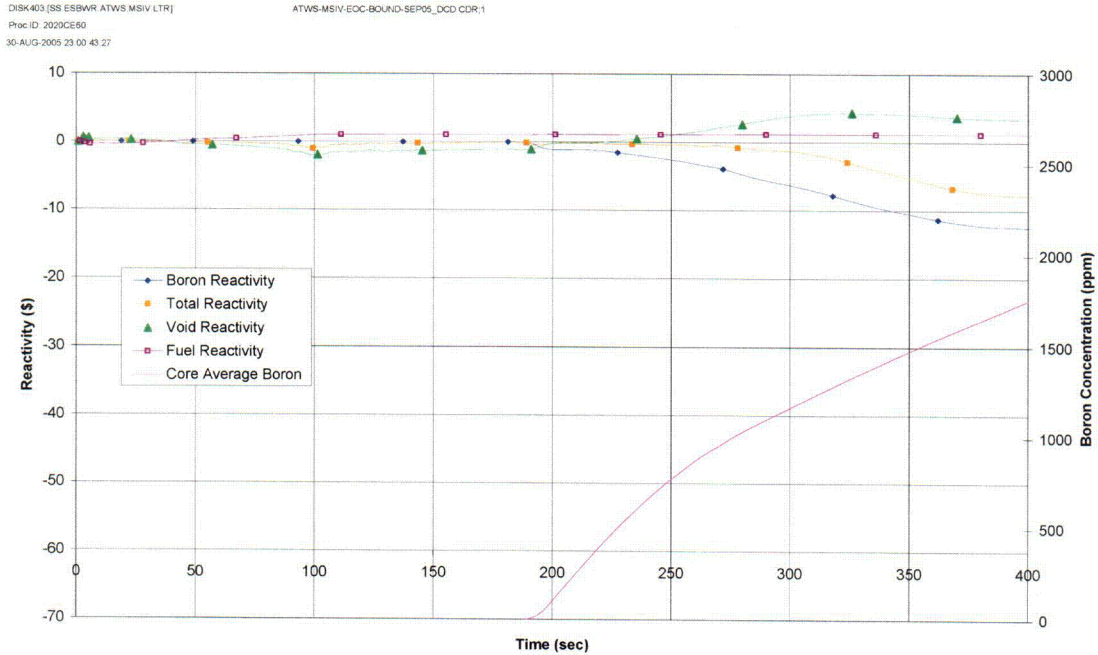**Figure 8.1-10. MSIVC Reactivity Feedback and Boron Concentration**
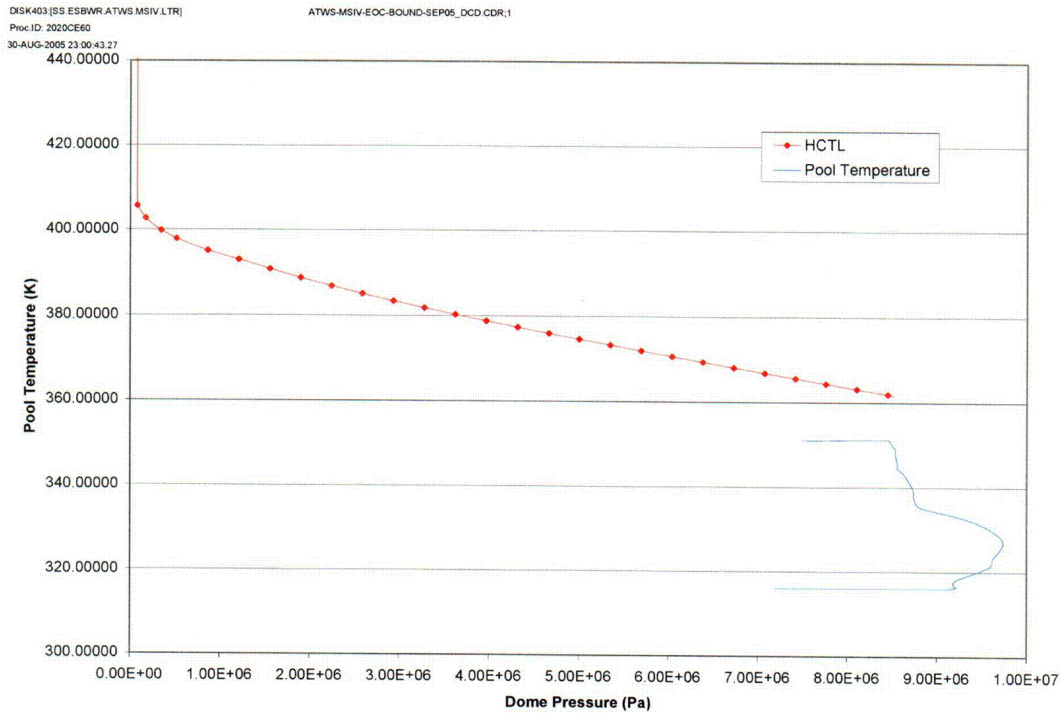
C05

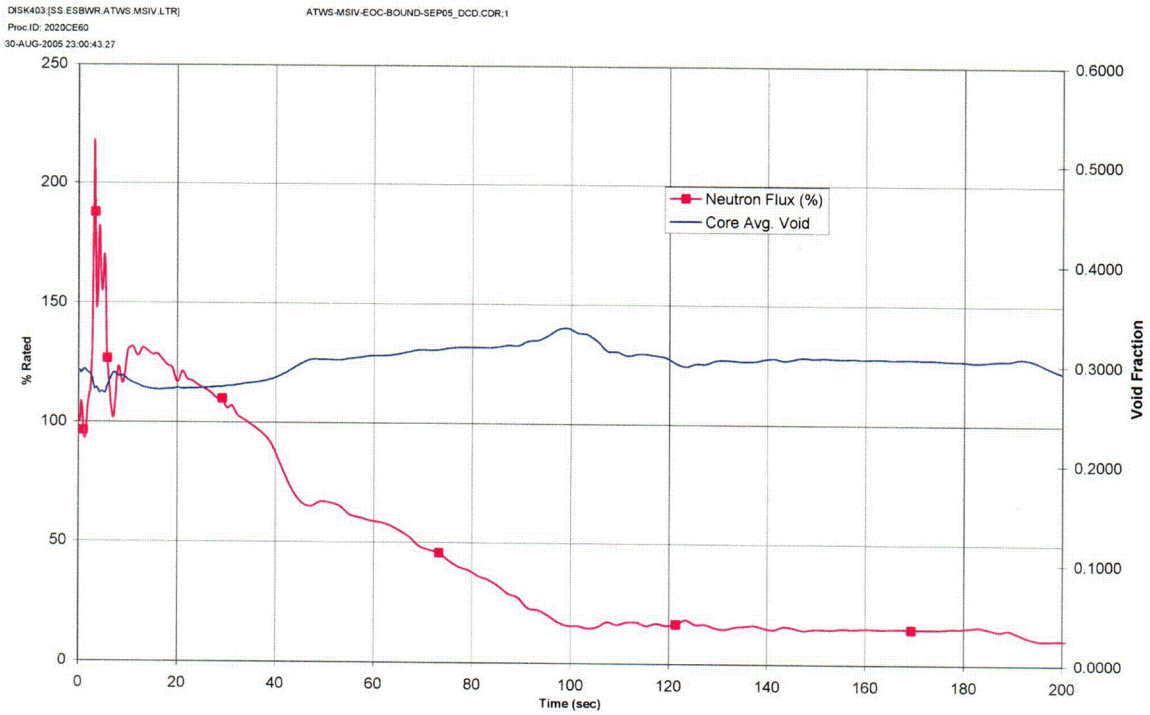**Figure 8.1-11. MSIVC HCTL and Pool Response**

Figure 8.1-12: MSIVC Neutron Flux and Core Average Void

8.1.2 Loss of Condenser Vacuum ATWS (LCV) Baseline Analysis

This transient starts with a turbine trip because of the low condenser vacuum; therefore, the beginning is the same as the turbine trip event. However, the MSIVs and turbine bypass valves also close after the condenser vacuum has further dropped to their closure setpoints. Hence, this event is similar to the MSIV closure event for all the key parameters. Table 8.1-6 shows the sequence of events for this transient.

Table 8.1-6. Sequence of Events for LCV

Time (s)	Event
0	Loss of Condenser Vacuum
0	Turbine Trip initiated and bypass opening
6	Bypass valves start to close, MSIVs close shortly thereafter.
8	Feedwater runback initiated
8	IC initiation
10	ATWS trip set at high pressure
11	SRVs open
26	Suppression pool cooling starts
26	Feedwater runback complete
49	Level drops below L2 set point
59	HPCRD flow starts
195	SLCS injection starts add reactor shutdown time, and time of max pool temp to all SOE tables
318	Peak Pool Temperature
390	Hot Shutdown achieved
716	High pressure design volume of borated solution injected into bypass

The key results from this analysis are presented in Table 8.1-7. and Figures 8.1-13 through 8.1-20. The results for the LCV case are very similar to those in the MSIVC case.

Table 8.1-7. Key Results for LCV

Parameter	Value	Time
Maximum Neutron Flux, %	218	9s
Maximum Vessel Bottom Pressure, MPaG (psig)	9.82(1425)	37s
Maximum Bulk Suppression Pool Temperature, °C (°F)	78.8(173.9)	318s
Associated Containment Pressure, MPaG (psig)	0.195(28.22)	318s
Peak Cladding Temperature, °C (°F)	915.3(1679.5)	31s

Figure 8.1-13. LCV Neutron Flux and Feed water Flow

Figure 8.1-14. LCV Steam Flow

Demonstration Analysis

DISK213:[SS.ESBWR.ATWS.LCV]
Proc.ID: 2020E897
26-OCT-2005 13:39:13.50   ATWS-LCV-EOC-BOUND-R11_DCD.CDR;1
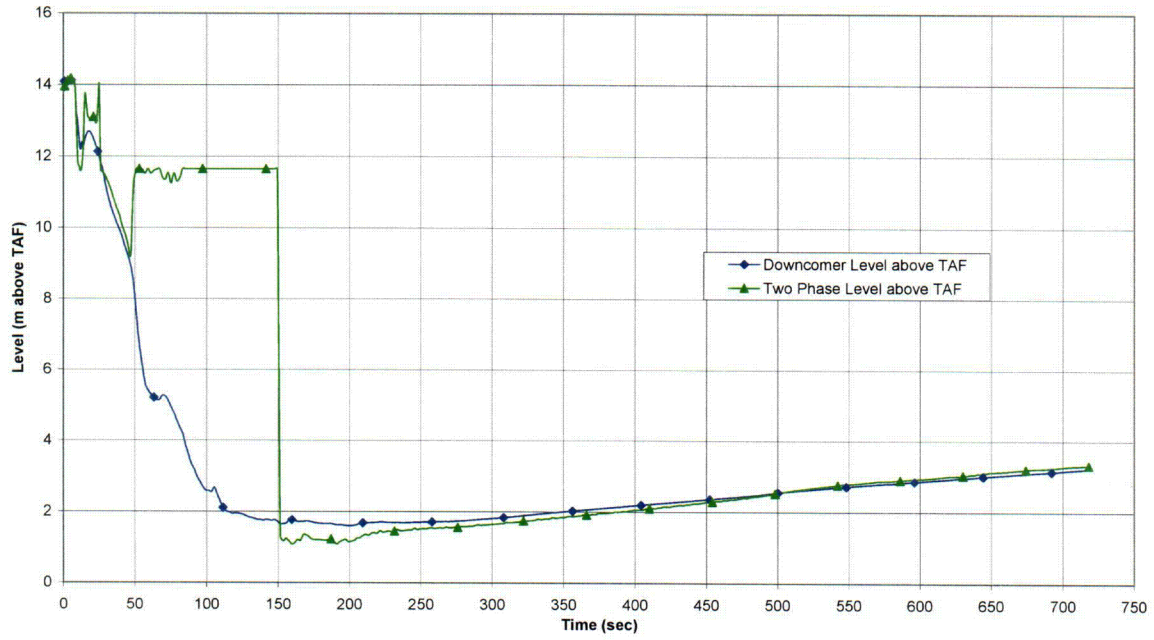
Figure 8.1-15. LCV Water Level

DISK213:[SS.ESBWR.ATWS.LCV]
Proc.ID: 2020E897
26-OCT-2005 13:39:13.50   ATWS-LCV-EOC-BOUND-R11_DCD.CDR;1
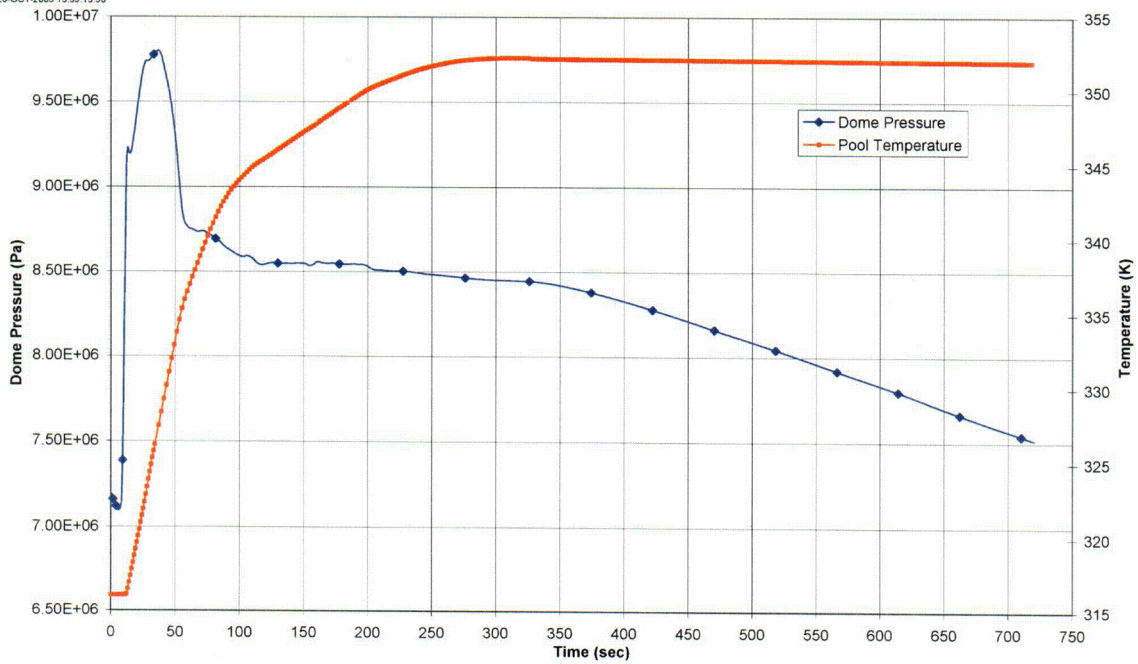
Figure 8.1-16. LCV Dome Pressure and Pool Temperature

DISK213.[SS.ESBWR.ATWS.LCV]
Proc.ID: 2020E897
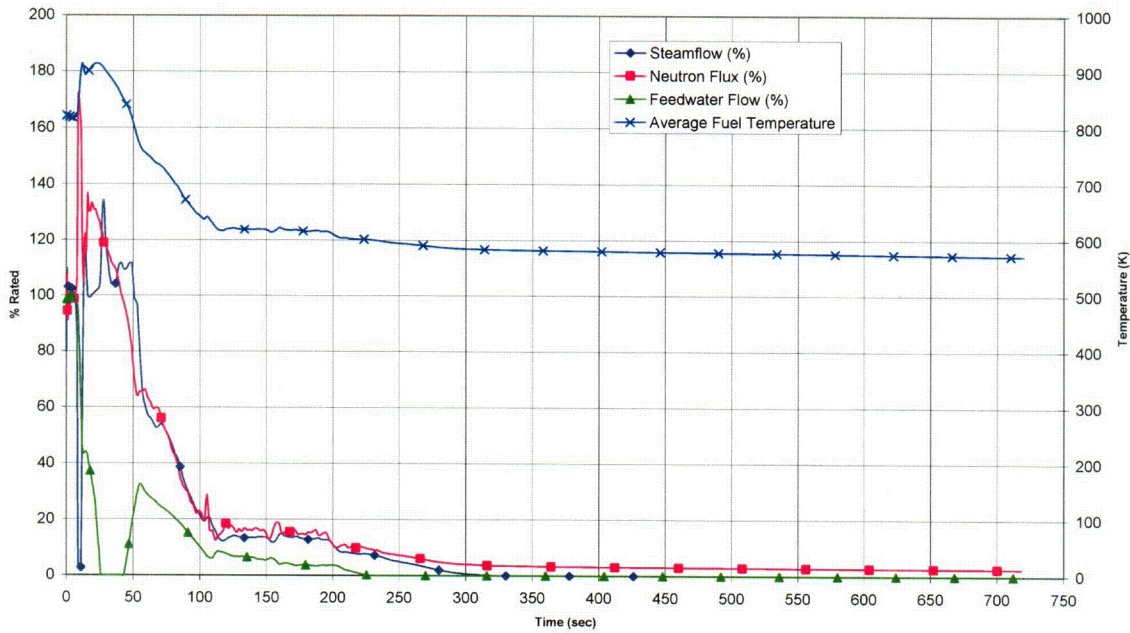26-OCT-2005 13:39:13.50

ATWS-LCV-EOC-BOUND-R11_DCD.CDR;1
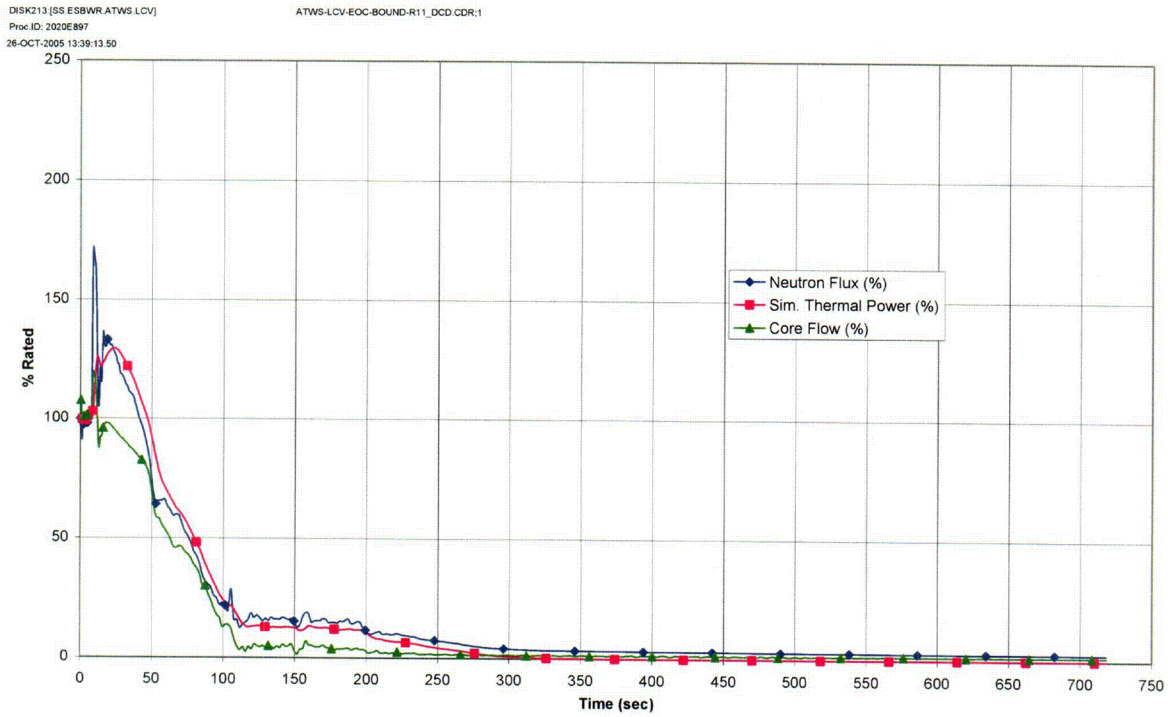
Figure 8.1-17. LCV Neutron Flux and Core Flow

DISK213.[SS.ESBWR.ATWS.LCV]
Proc.ID: 2020E897
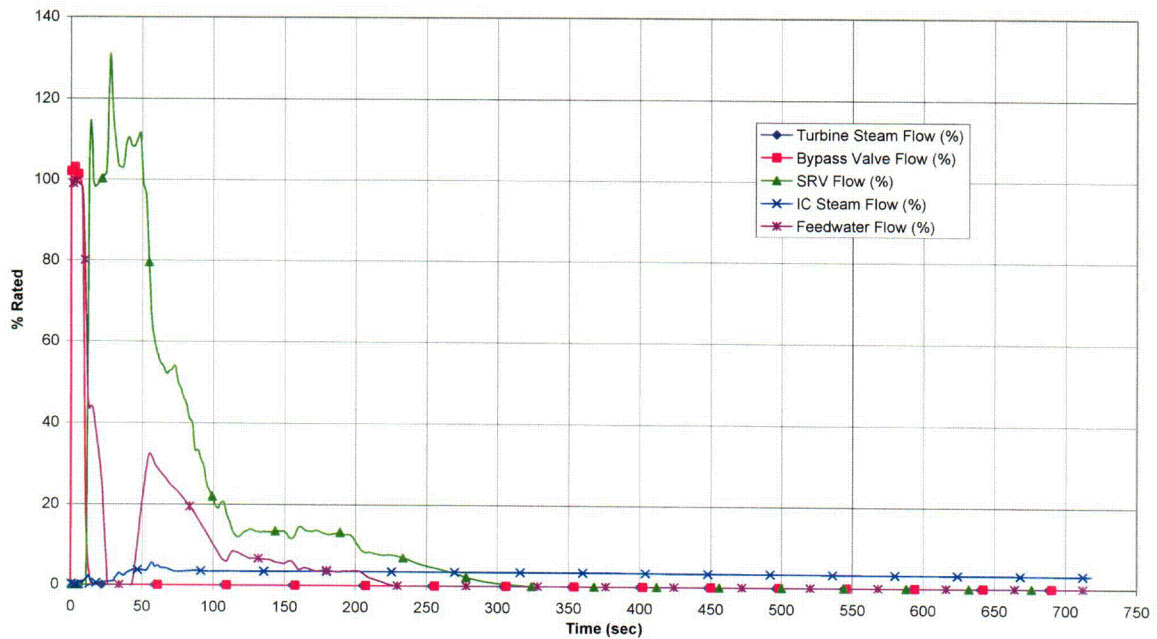26-OCT-2005 13:39:13.50

ATWS-LCV-EOC-BOUND-R11_DCD.CDR;1
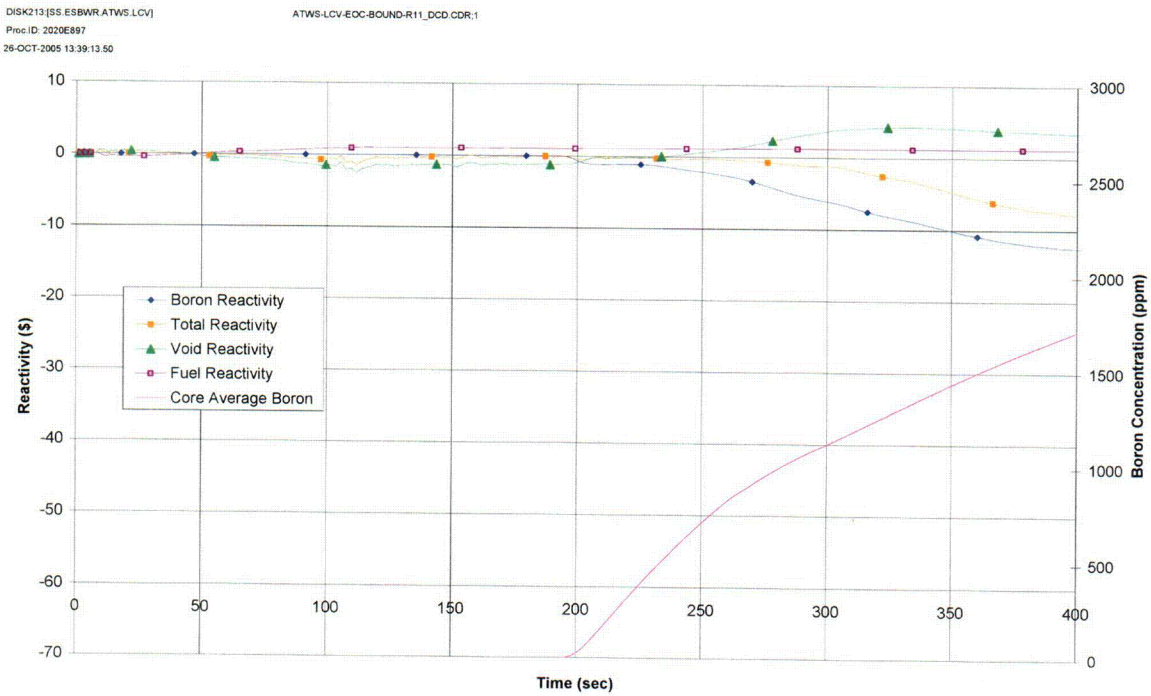
Figure 8.1-18. LCV Reactivity Feedback and Core Average Boron

C09

Demonstration Analysis

DISK213:[SS.ESBWR.ATWS.LCV]
Proc.ID: 2020E897
26-OCT-2005 13:39:13.50 — ATWS-LCV-EOC-BOUND-R11_DCD.CDR;1
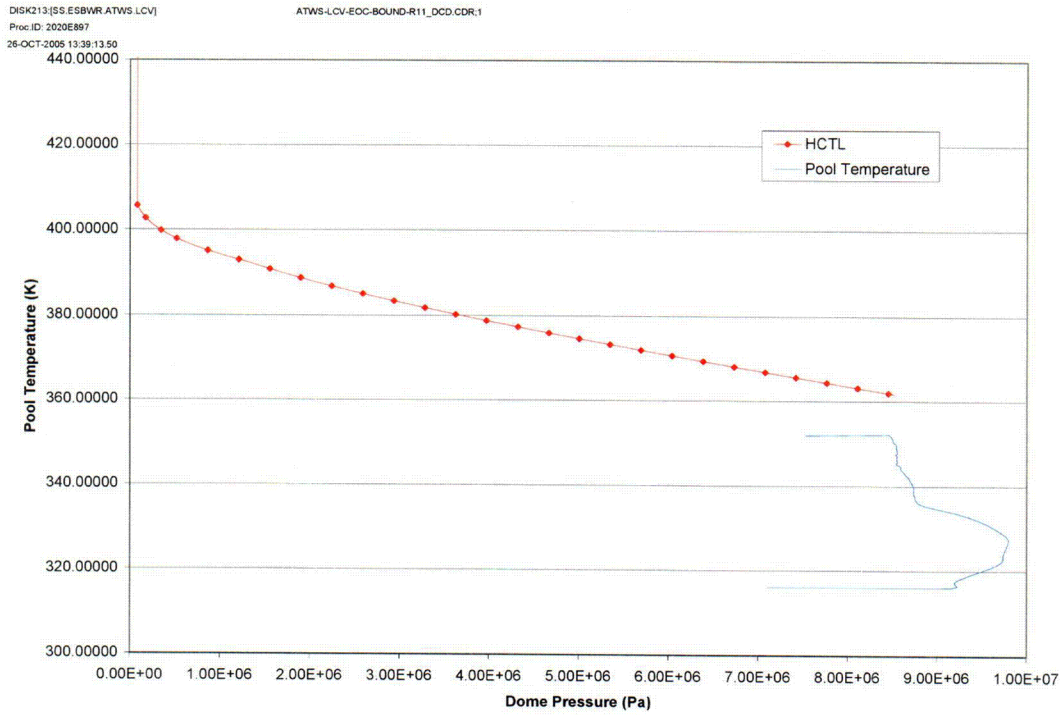
Figure 8.1-19. LCV HCTL and Pool Response

DISK213:[SS.ESBWR.ATWS.LCV]
Proc.ID: 2020E897
26-OCT-2005 13:39:13.50 — ATWS-LCV-EOC-BOUND-R11_DCD.CDR;1

Figure 8.1-20. LCV Neutron Flux and Core Average Void

8.1.3 Loss of Feedwater Heating ATWS (LFWH) Baseline Analysis

This transient does not trip any automatic ATWS logic. As a result of the loss of feedwater heating, the reactor power increases and settles into a new steady state. It is assumed that the operator initiates ARI at approximately 10 minutes after the beginning of this event to shut the reactor down. However, the feedwater runback initiated by manual ARI signal and APRM not-downscale signal causes the water level to drop below Level 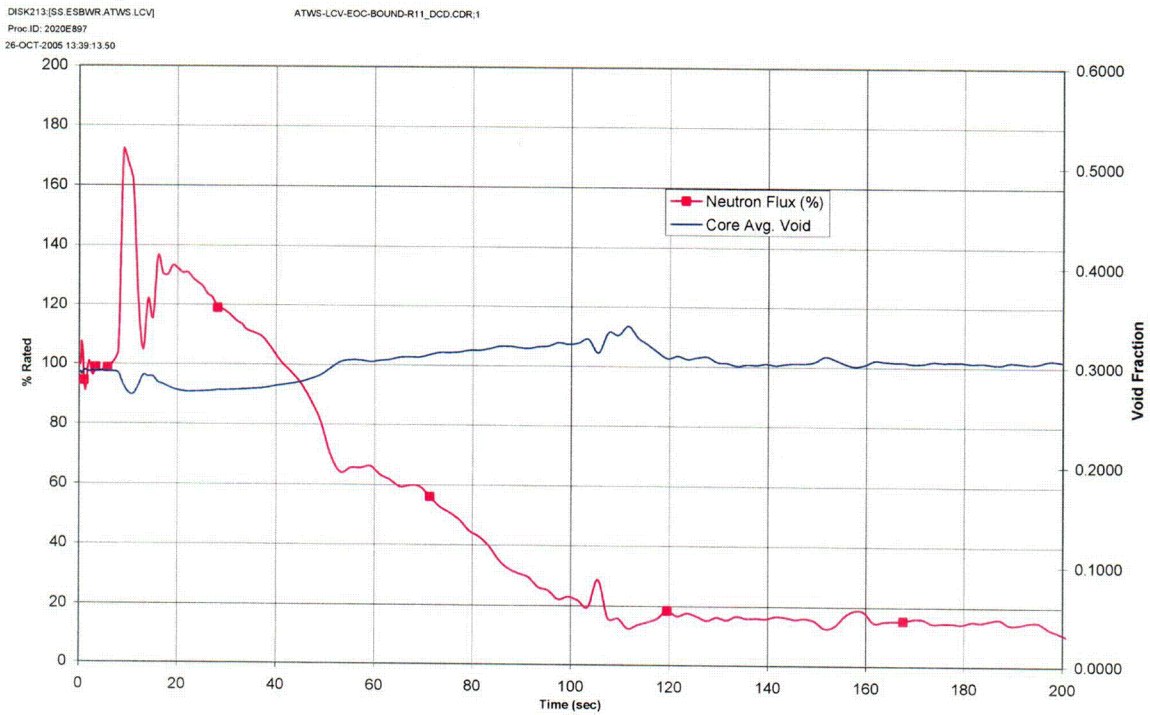2. Low water level results in a closure of all MSIVs, and subsequent reactor pressure increase. The pressure increase is mitigated by SRV opening. The initiation of the ATWS logic sets the SLCS timer. Upon failure of rod insertion, the SLCS initiates at about 13 minutes into the transient and the reactor is brought to a hot shutdown condition in can bring the reactor to the hot shutdown condition in little over 15 minutes after the event starts.

The sequence of events for this transient is presented in Table 8.1-8. Results are presented in Table 8.1-8 and Figures 8.1-21 through 8.1-28. The comparison of these results with the MSIVC and LCV cases indicate that this transient is not limiting for any of the key parameters.

Table 8.1-8. Sequence of Events for LFWH

Time (s)	Event
0	Loss of Feedwater heating
600	Feedwater runback initiated
618	Feedwater runback completed
638	L2 setpoint reached
648	HPCRD flow starts
668	MSIV closure starts
670	IC initiation
692	SRVs open
785	SLCS flow starts
796	Suppression pool cooling starts
880	Peak Pool Temperature
926	Hot Shutdown achieved
1302	High pressure design volume of borated solution injected into bypass

Table 8.1-9. Key Results for LFWH

Parameter	Value	Time
Maximum Neutron Flux, %	120	596s
Maximum Vessel Bottom Pressure, MPaG (psig)	8.62(1250)	693s
Maximum Bulk Suppression Pool Temperature, °C (°F)	50.0(122.0)	880s
Associated Containment Pressure, MPaG (psig)	0.141(20.46)	880s
Peak Cladding Temperature, °C (°F)	316.0(600.8)	620s

DISK213:[SS.ESBWR.ATWS.LFWH]
Proc.ID: 2020F09A
26-OCT-2005 13:43:10.84

ATWS-LFWH-EOC-BOUND-R11_DCD.CDR;1
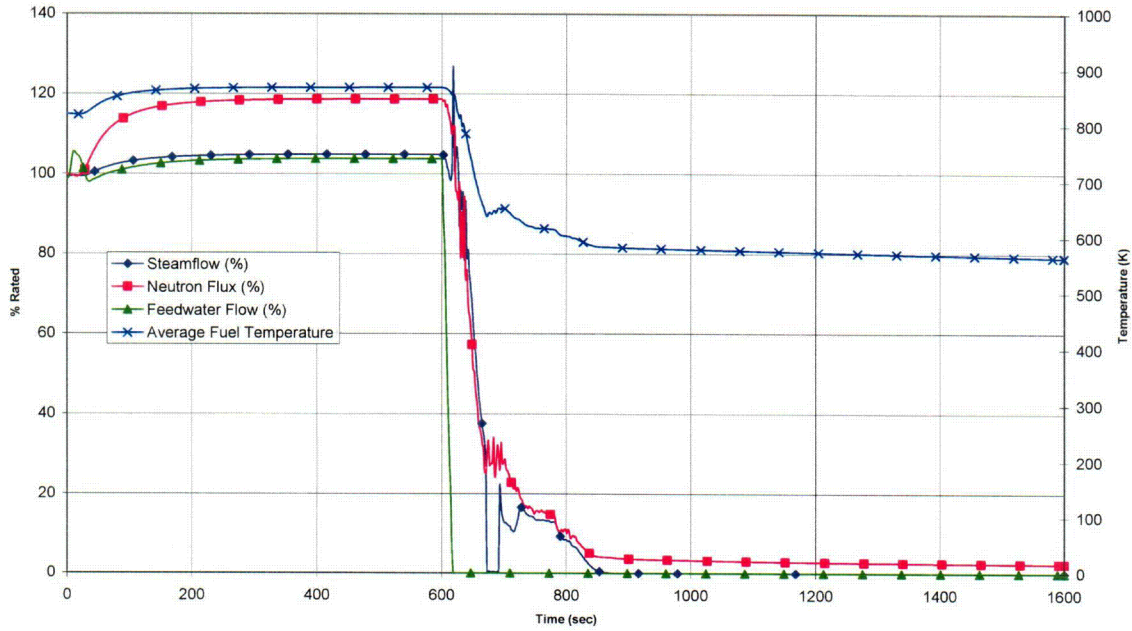
Figure 8.1-21. LFWH Neutron Flux and Feedwater Flow

DISK213:[SS.ESBWR.ATWS.LFWH]
Proc.ID: 2020F09A
26-OCT-2005 13:43:10.84

ATWS-LFWH-EOC-BOUND-R11_DCD.CDR;1
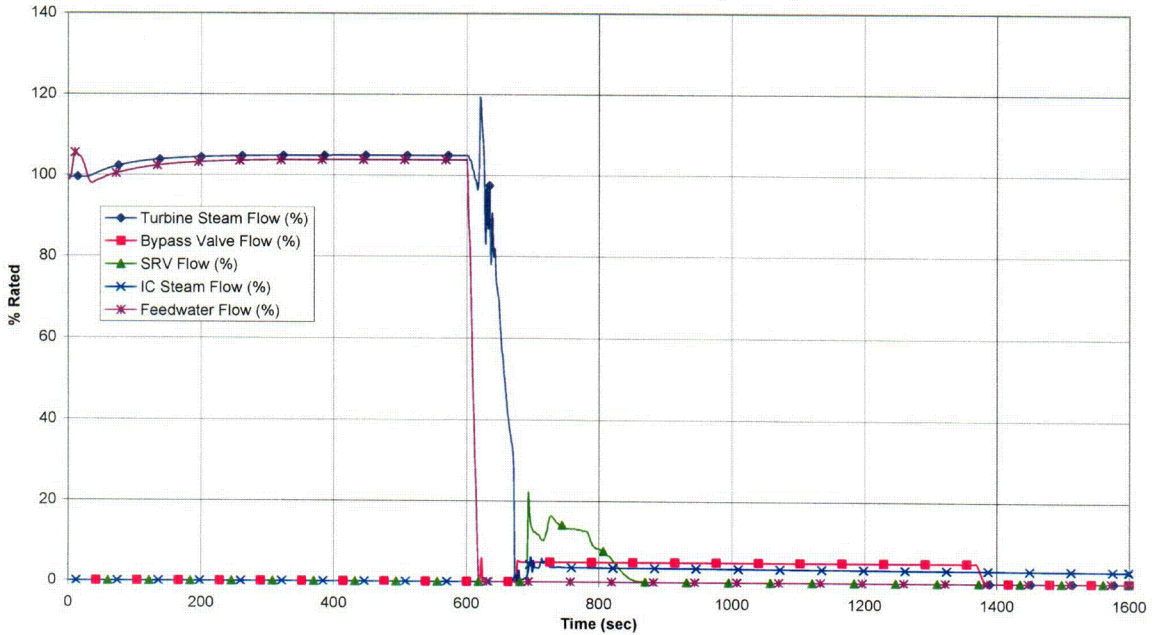
Figure 8.1-22. LFWH Steam Flow

Demonstration Analysis

DISK213:[SS.ESBWR.ATWS.LFWH]
Proc.ID: 2020F09A
26-OCT-2005 13:43:10.84   ATWS-LFWH-EOC-BOUND-R11_DCD.CDR;1
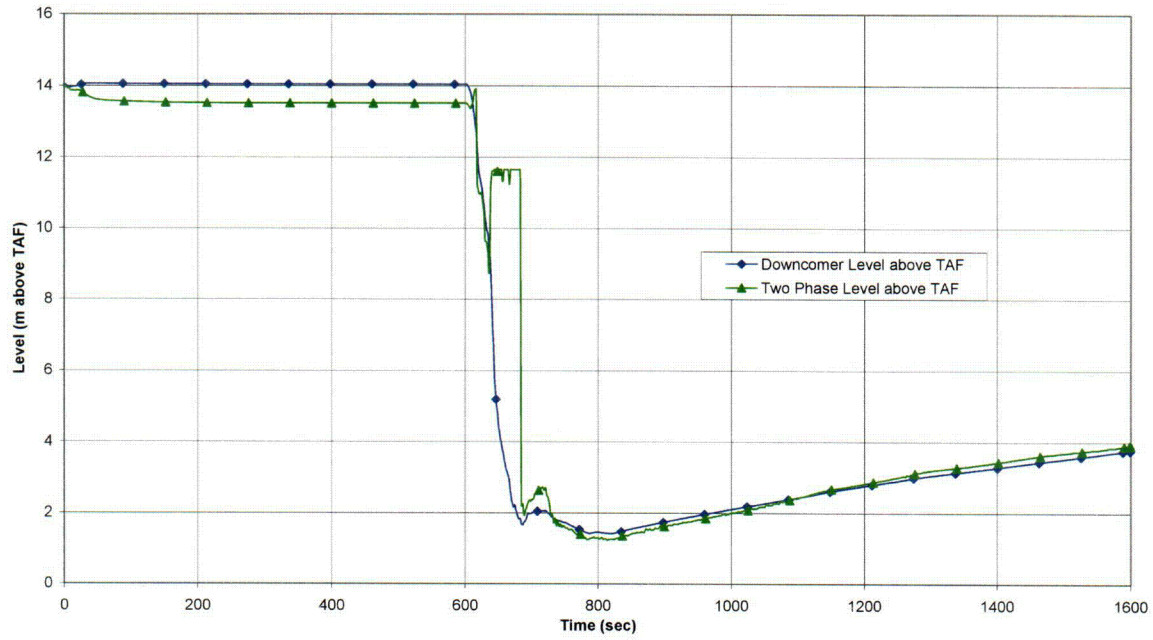
Figure 8.1-23. LFWH Water Levels

DISK213:[SS.ESBWR.ATWS.LFWH]
Proc.ID: 2020F09A
26-OCT-2005 13:43:10.84   ATWS-LFWH-EOC-BOUND-R11_DCD.CDR;1
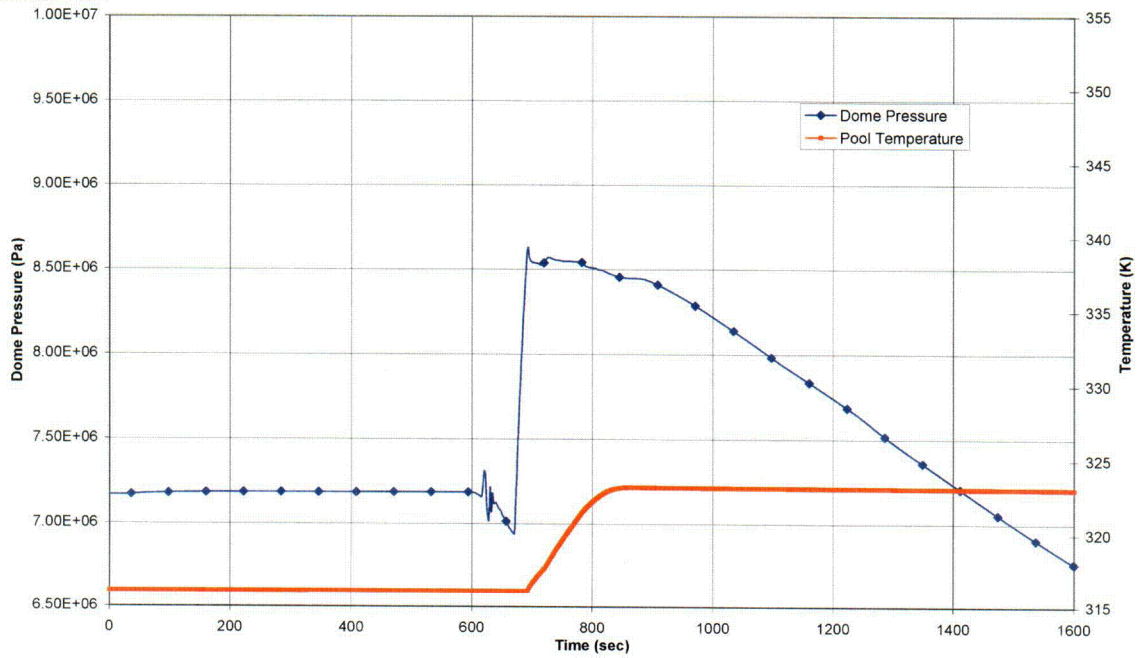
Figure 8.1-24. LFWH Pressure and Pool Temperature

C12
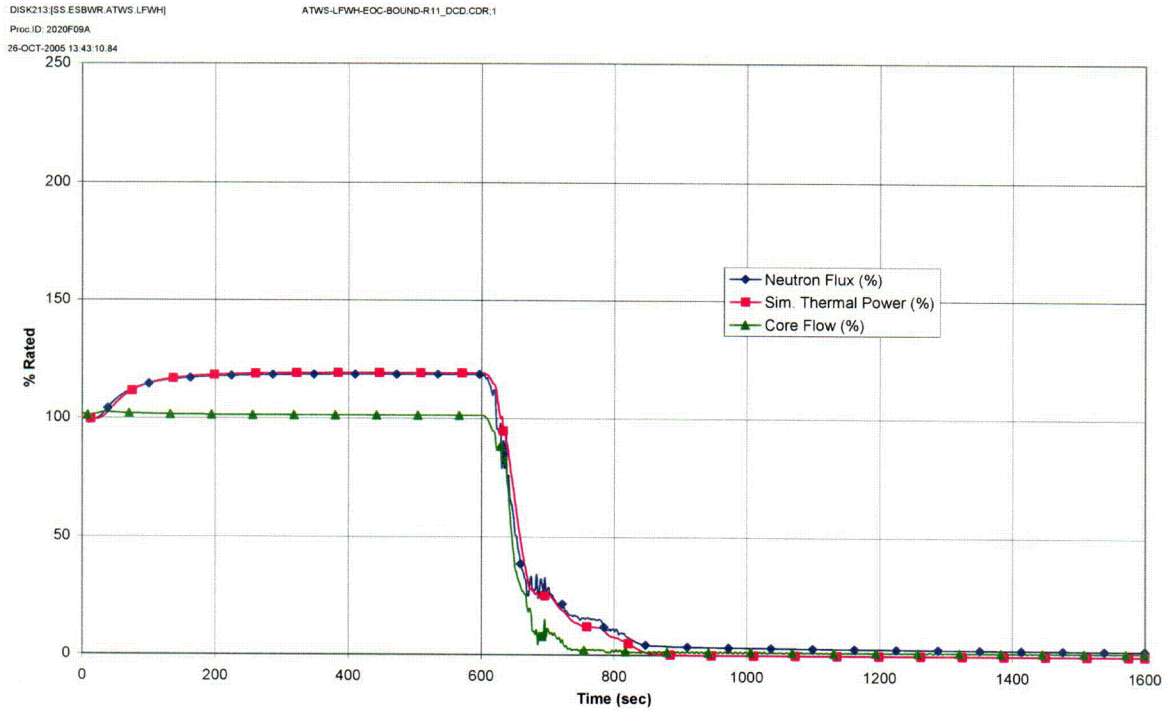
Figure 8.1-25. LFWH Neutron Flux and Core Flow
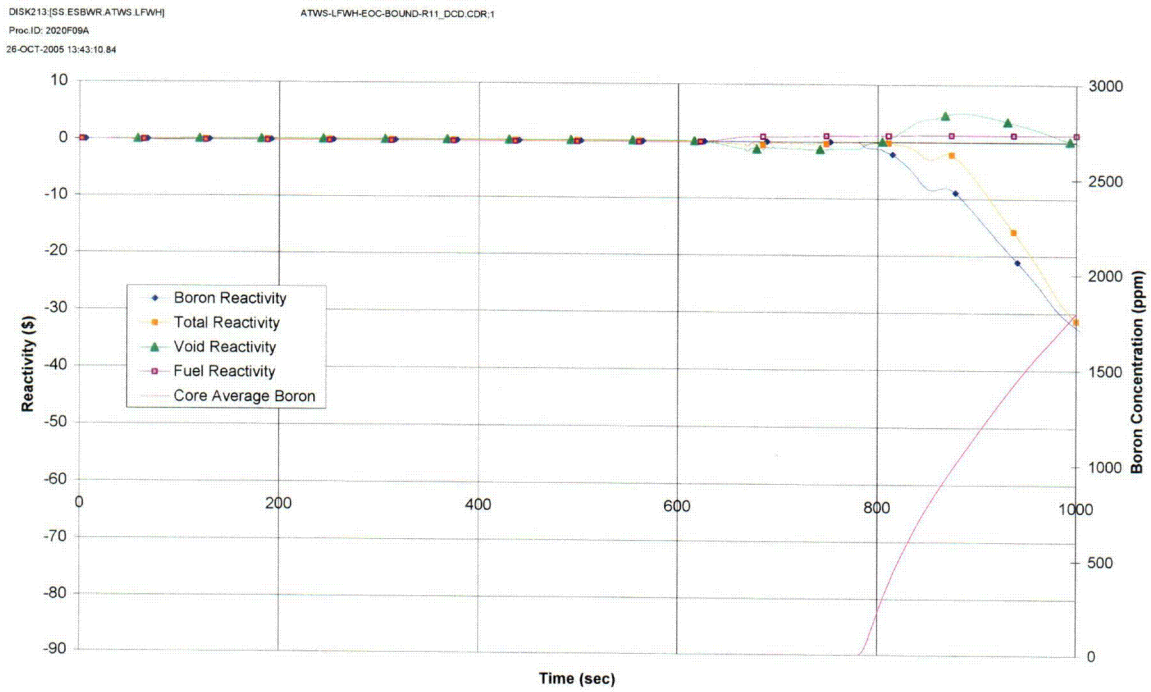
Figure 8.1-26. LFWH Reactivity Feedback and Core Average Boron

Demonstration Analysis
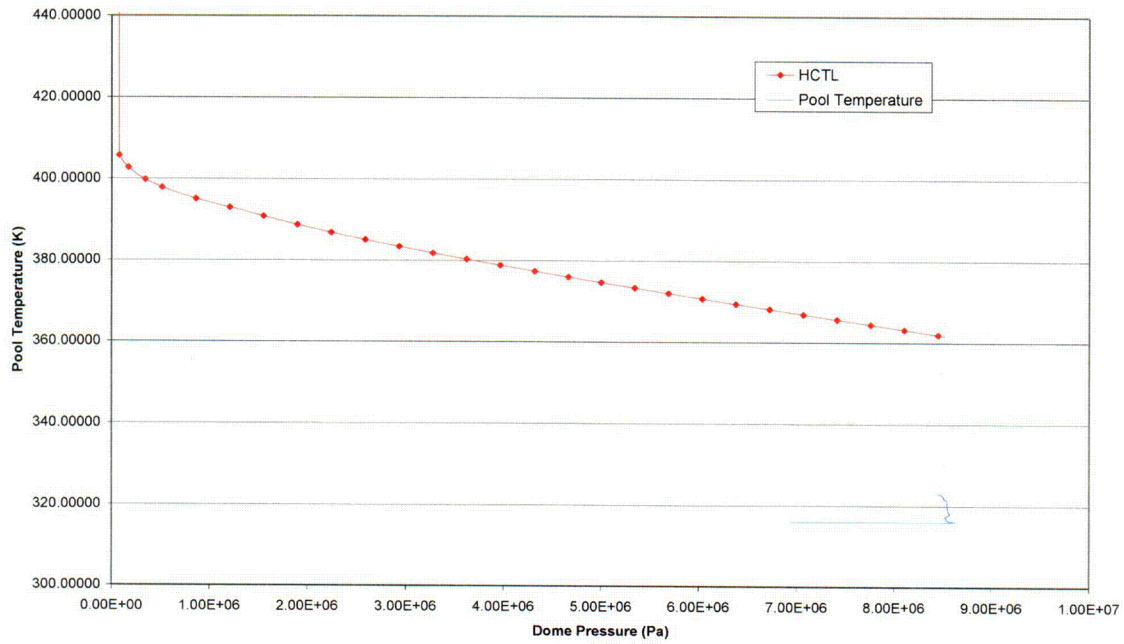
Figure 8.1-27. LFWH HCTL and Pool Response
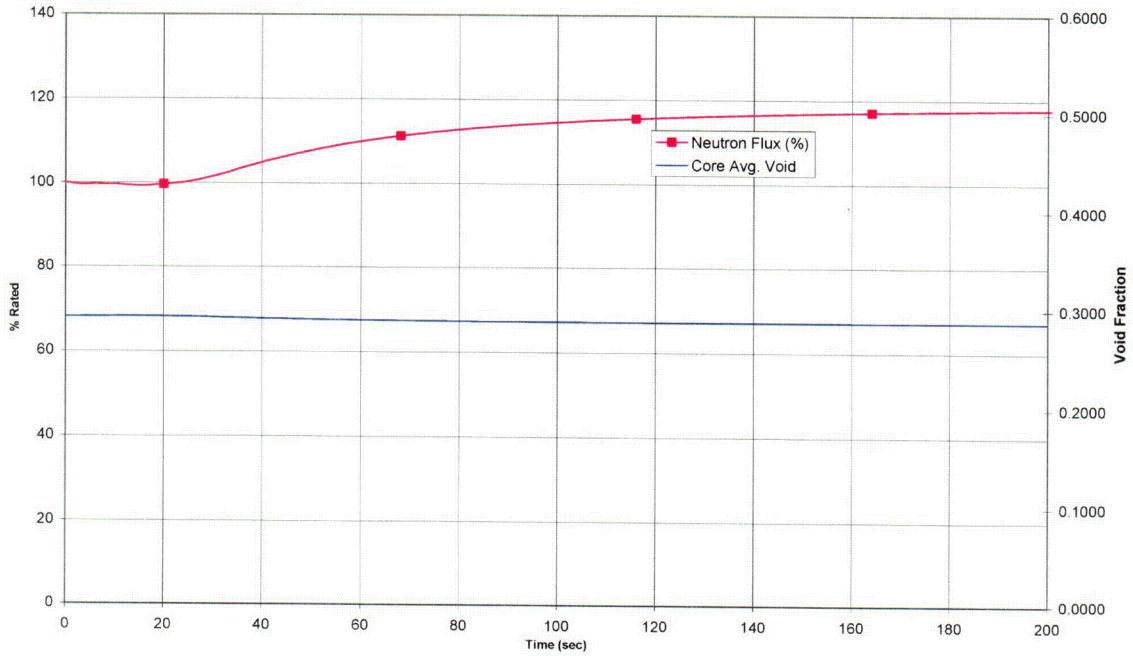
Figure 8.1-28. LFWH Neutron Flux and Core Average Void

Demonstration Analysis

8.2 Initial Condition and Plant Parameter Review

8.2.1   Initial Conditions

This section will consider the sensitivity of the limiting MSIVC ATWS case to initial conditions in the plant. Table 8.2-1 summarizes the initial condition sensitivity analyses performed as part of this study. The critical parameters studied are peak pressure, peak clad temperature, peak suppression pool temperature, and peak power.

Table 8.2-1. Initial Conditions Sensitivity Analysis

8.2.1.1   Initial Conditions Sensitivity Results

A summary of the sensitivity analysis for the MSIVC transient is provided in 8.2-2. . The sensitivity analyses were performed at BOC and the changes in various parameters as a result of initial condition uncertainties are discussed in this subsection.
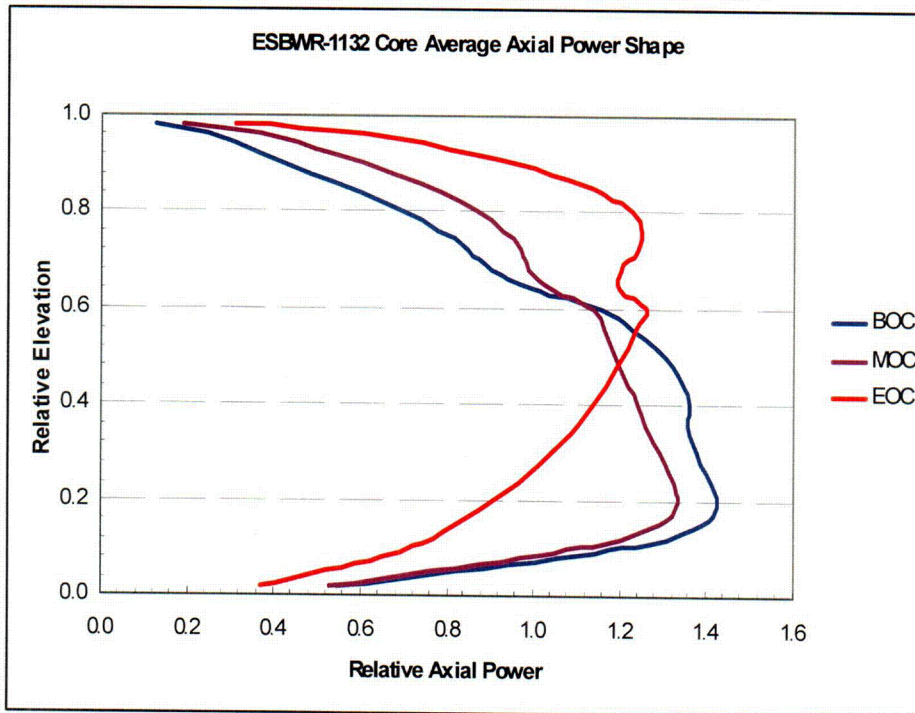
Figure 8.2-1. Relative Axial Power Distribution for Three Exposure Statepoints

C15

Table 8.2-2. MSIVC Allowable Operating Range Results: Change from Base Case

[[Proprietary Information Redacted]]

The characterization of these results is presented in Table 8.2-3.

Table 8.2-3. MSIVC Initial Conditions Characterizations

[[Proprietary Information Redacted]]

8.2.2 Plant Parameters

As described in Section 8.1, plant parameters like S/RV capacity, MSIV stroke time, and IC capacity have been conservatively modeled in the baseline analyses. This section details the studies undertaken to determine the impact of other plant parameters that have a direct impact on one or more of the critical safety related parameters during an ATWS event. The sensitivity analyses were performed at BOC and the changes in various parameters as a result of plant parameter uncertainties are discussed in this subsection.

Table 8.2-4 presents the set of plant parameters studied with a description of how each parameter was different from the baseline analysis.

Table 8.2-4. MSIVC Plant Parameters

Plant Parameter	Base Case	Sensitivity Case	Purpose/Remarks
Lower EOP ATWS Water Level	TAF + 1.524m	TAF	Impact on pool temperature
Higher EOP ATWS Water Level	TAF + 1.524m	TAF + 3.048m	Impact on pool temperature
Boron Enrichment	94% in B-10	19.8% in B-10	Impact on pool temperature
FAPCS	On	Off	Impact on pool temperature
SLCS flow velocity at nozzle	Time dependent flow based on accumulator depressurization	Constant flow of 30.5m/s	Impact on shutdown time
SRV Capacity*	Tech Spec	Nominal	Impact on Pressure, pool temperature
IC	Full IC Capacity	75% IC capacity	Impact on pool temperature
Suppression	No opening of S/RVs at SLCS	S/RVs open at SLCS	Determine whether reactor would be critical

Pool HCTL	initiation	initiation, (simulates pool reaching HCTL at the start of boron injection).	after a depressurization if the HCTL curve were reached.

* See Section 8.3 for more information

8.2.2.1 Plant Parameter Sensitivity Results

Table 8.2-5 presents results from the plant parameter sensitivity studies.

Table 8.2-5. MSIVC Plant Parameter Sensitivity Study, Change from Base Case (% change from Base)

[[Proprietary Information Redacted]]

The peak power was not sensitive to any of the plant parameters. Increasing the SRV capacity from the nameplate value to the nominal value (approximately 8%), decreased the peak pressure by about [[Proprietary Information Redacted]] and the PCT by [[Proprietary Information Redacted]]. Corresponding to this, the peak pool temperature increased by [[Proprietary Information Redacted]] and the containment pressure by [[Proprietary Information Redacted]]. Changes to the other plant parameters had very little effect on the key quantities. For the depressurization case, the high pool temperature is caused by dumping energy from the RPV into the pool and the reactor remains subcritical at the low pressure.

Additional cases, with and without depressurization, where the vessel was refilled to the normal water level over a period of one half hour after the termination of SLCS flow, did not lead to recriticality of the system.

[[Proprietary Information Redacted]] A case with natural boron as opposed to the 94% enriched boron used in the plant indicated that the shut down takes about [[Proprietary Information Redacted]] minutes longer, for a total of [[Proprietary Information Redacted]] minutes from the initiation of the SLCS.

8.2.3 ATWS Stability Study

The MSIVC baseline model was used to determine if any power instabilities set in during the transient. The case was run in for full transient for 720s without introducing any specific perturbation to the system. The stability studies were performed using the explicit first order integration method for the solution in all the channel components in contrast to the implicit mode used in the baseline analysis. In addition, two cases were run starting at points where the power to flow ratio was high but fairly constant. In these two cases the inlet liquid velocities in the channels were increased by 5% to introduce perturbations to the system. The first case was started at 25s and run for 20s and the second case was started at 185s and run for 35s. Figures 8.2-2, 8.2-3, and 8.2-4 show the power for the three cases. These plots show the comparison of the power profile for the baseline case (indicated as implicit) and the stability run (indicated as explicit). The effects of the perturbations were damped out in both cases and did not lead to growing oscillations.

These plots indicate that stability is not an issue during an ATWS event in ESBWR.

[[Proprietary Information Redacted]]
Figure 8.2-2. MSIVC Stability Power Comparison
[[Proprietary Information Redacted]]
Figure 8.2-3. MSIVC Stability Power Comparison: 25s

[[Proprietary Information Redacted]]
Figure 8.2-4. MSIVC Stability Power Comparison: 185s

8.2.4 Summary of Initial Conditions, Plant Parameters and Stability

The following can be concluded based on the initial condition, plant parameter, and stability analyses results:

- Peak power and peak PCT are limiting for the EOC condition. Other critical parameters are not sensitive to the initial conditions. Clad oxidation is insignificant in all cases.

- The peak suppression pool temperature is reached at 254s for the MSIVC case.

- Core stability is maintained during ATWS.

- The pool heat up is impacted primarily by the core power and the SR/V steam flow before the water level is reduced by FW runback to the EOP specified level, and secondarily the core power and steam flow after level reduction. The response after SLCS injection does not have a strong effect on pool temperature.

- The analyses indicate that none of the critical parameters exceeds safety limits and the plant achieves shutdown conditions safely.

8.3 Uncertainty Analysis for Licensing Events

The uncertainty analysis is performed for the highly ranked phenomena and initial conditions as discussed in Section 3 of this report. The effects of the uncertainty associated with these phenomena on peak vessel and containment pressure, PCT, peak pool temperature and the peak power for the MSIVC case are examined in this section.

Using the estimated deviations from the base case obtained from the uncertainty analyses, an overall uncertainty for these key parameters is obtained and added to the respective values obtained in the nominal case.

8.3.1 Uncertainty Screening

Analyses have been performed at both the +1 σ and -1 σ level for each of the model uncertainties and initial conditions (some of these results have been discussed in Section 8.2). Figures 8.3-1 through 8.3-5 present these results.

[[Proprietary Information Redacted]]

Figure 8.3-1. MSIVC –Peak Power Sensitivity

[[Proprietary Information Redacted]]

Figure 8.3-2. MSIVC –Peak Vessel Pressure Sensitivity

[[Proprietary Information Redacted]]

Figure 8.3-3. MSIVC –Peak Clad Temperature Sensitivity

[[Proprietary Information Redacted]]

Figure 8.3-4. MSIVC –Peak Pool Temperature Sensitivity

[[Proprietary Information Redacted]]
Figure 8.3-5. MSIVC –Peak Containment Pressure Sensitivity

The peak power is sensitive to an increase in the interfacial shear in the core to the extent of [[Proprietary Information Redacted]] with the parameter remaining insensitive to all other phenomena. The dome pressure is within [[Proprietary Information Redacted]] of the peak value in the base case for all phenomena. The PCT is the most sensitive parameter and is impacted by the total power, GEXL critical quality, feedwater enthalpy, interfacial shear in the core, vapor side interfacial heat transfer, spacer loss coefficient, downcomer and upper plenum interfacial drag coefficient, and rewet quality margin. The peak pool temperature and peak containment pressure are insensitive to the application of uncertainties to the various phenomena.

8.3.2 Overall Uncertainty

The overall uncertainty applicable to each of the parameters is obtained by taking the square root of the sum of squares of the difference between the base case and the PIRT phenomena that changed these parameters in a positive sense. The uncertainty for each parameter is then compared to the difference between the values for these parameters for a bounding case when compared to a nominal case. Any excess uncertainty over this difference is added as a bias to the bounding case .

Following the uncertainty analyses, a further set of conservatisms in the form of initial condition uncertainties was added to the original bounding case viz. 102% power, 0.125 MPa lower dome pressure setpoint, and an approximate 5% increase in feedwater enthalpy. Since the containment parameters showed more conservatism when the nominal SRV capacity was used in the analyses, a separate bounding analysis was performed for the containment with a S/R valve capacity that was 7.8% above the nominal capacity. The value 7.8% represents the difference between the TS capacity and the nominal capacity.

Table 8.3-1 outlines the main differences in the three cases.

Table 8.3-1. Main Features of the Nominal, and Bounding Cases

[[Proprietary Information Redacted]]

A summary of the results for the nominal and bounding cases is presented below in Table 8.3-2.

Table 8.3-2. Nominal and Bounding Cases: Summary

[[Proprietary Information Redacted]]

The overall uncertainty associated with each parameter was obtained as described above. Table 8.3-3 presents differences between the nominal and the other two cases as well as any bias to be applied. Finally, Table 8.3-4 presents bounding numbers and their comparison to the design limits.

Table 8.3-3 Summary of Uncertainty Analyses

[[Proprietary Information Redacted]]

Table 8.3-4. Final Results with applied Bias

[[Proprietary Information Redacted]]

The biases in the peak pool temperature and containment pressure are less than two percent of the peak values and are thus within the noise level of the analyses. All the key parameters in the bounding case are within design limits.

9.0 CONCLUSIONS

- TRACG is capable of simulating ESBWR ATWS events. It models the important phenomena, and the models of the important phenomena are qualified.

- An application methodology is defined for ESBWR ATWS analysis. The procedure for performing the calculation considers specific modeling applied in the code qualification for ESBWR.

- The nominal TRACG calculation, combined with bounding initial conditions and plant parameters, produces an overall conservative estimate of ATWS peak vessel pressure and peak fuel clad temperature.

- A conservative value of suppression pool temperature is achieved including an adder based on the combined uncertainties at the 1-sigma level.

10.0 REFERENCES

[1]   B. S. Shiralkar and Y. K. Cheung, <u>TRACG Application for ESBWR, NEDC-33083</u>-PA, March 2005

[2]   *United States Nuclear Regulatory Commission Standard Review Plan* – NUREG 0800, 15.8, Rev 1, July 1981.

[3]   *Assessment of BWR Mitigation of ATWS*, NEDE-24222 (Volume 2). December, 1979.

[4]   *Qualification of the One-Dimensional Core Transient Model for Boiling Water Reactors*, NEDO-24154-A and NEDE-24154-P-A, Volumes I, II and III. August 1986.

[5]   *Qualification of the One-Dimensional Core Transient Model for Boiling Water Reactors*, NEDO-24154-P-A (Supplement 1 – Volume 4), Revision 1. February, 2000.

[6]   B. Boyack, et al., *Quantifying Reactor Safety Margins: Application of Code Scaling, Applicability, and Uncertainty Evaluation Methodology to a Large-Break, Loss-of-Coolant Accident,* NUREG/CR-5249. December, 1989.

[7]   *General Electric Standard Application for Reactor Fuel (GESTAR II)*, NEDE-24011-P-A-14. June, 2000.

[8]   F. Bolger, et al., *TRACG Application for Anticipated Transient Without Scram Pressure Analyses*, NEDE-32906P Supplement 1 -A. November 2003.

[9]   *TASC-03A, A Computer Program for Transient Analysis of a Single Channel,* NEDC-32084P-A, Revision 2. July, 2002.

[10]   *Anticipated Transients Without Scram for Light Water Reactors*, NUREG-0460, Volumes 1, 2, 3. December, 1978.

[11]   J. G. M. Andersen, et al., *TRACG Qualification,* NEDE-32177P. January, 2000.

[12]   J. G. M. Andersen, et al., *TRACG Application for Anticipated Operational Occurrences Transient Analyses*, NEDE-32906P. January, 2000.

[13]   B. S. Shiralkar and R. E. Gamble, *ESBWR Test and Analysis Program Description*, NEDC-33079P, August 2002

[14]   J. G. M. Andersen, et al., *TRACG Model Description,* NEDE-32176P.

[15]   J. R. Fitch, et al., TRACG Qualification for SBWR (Licensing Topical Report), NEDC-32725P, September, 1997

[16]   B. S. Shiralkar and R.E. Gamble, *ESBWR Test and Analysis Program Description,* NEDC-33079P, Supplement 1, Revision 0, August 2002

[17]   J. R. Fitch, et al, NEDC-33080P, *TRACG Qualification for ESBWR,* Class III (GE Proprietary Information), dated August 2002.

[18]   S. A. Eide, et al., *Reliability Study: General Electric Reactor Protection System, 1984–1995,* NUREG/CR-5500, Vol. 3, INEL/EXT-97-00740, February 1999

[19]   B. S. Shiralkar, L. A. Klebanov, and Y. K. Cheung, NEDE-33083P Supplement 1, TRACG Application for ESBWR Stability Analysis, December 2004

[20]   K. T. Schaefer, NEDO-33175, Revision 1, Classification of ESBWR Abnormal Events and Determination of Their Safety Analysis Acceptance Criteria, February 2005

[21]   NEDO-30130-A, Steady State Nuclear Methods, April 1985.

[22]   S. Morooka, T. Ishizuka, M. Iizuka and K. Yoshimura, Experimental Study on Void Fraction in a Simulated BWR Assembly (Evaluation of Cross-Sectional Averaged Void Fraction), Nuclear Engineering and Design 114, pp. 91-98 (1989).

[23]   T. Mitsutake, S. Morooka, K. Suzuki, S. Tsonoyama and K. Yoshimura, Void Fraction Estimation within Rod Bundles Based on Three-Fluid Model and Comparison with X-Ray CT Void Data, Nuclear Engineering and Design 120, pp. 203-212 (1990).

[24]   P. Saha and N. Zuber, Point of Net Vapor Generation and Vapor Void Fraction in Subcooled Boiling, Proceedings of the 5th International Heat Transfer Conference, Tokyo 1974.

[25]   NEDO-23785-1-A, Rev. 1, The GESTR-LOCA and SAFER Modes for the Evaluation of the Loss-of-Coolant Accident, Vol. 1: GESTR-LOCA – A Model for the Prediction of Fuel Rod Thermal Performance.

[26]   Supplemental Information for Plant Modifications to Eliminate Significant In-Core Vibrations", NEDE-21156, Jan 1976

[27] B. S. Shiralkar and R. E. Gamble, "ESBWR Test and Analysis Program Description", NEDC-33079P, August 2002 (section 3.3).

[28] J. P. Walkush, "High Pressure counterflow CHF", EPRI Report 292-2, January 1975

[29] V. P. Carey, Liquid-Vapor-Phase-Change Phenomena, Hemisphere Publishing, 1992.

[30] R. E. Dimenna, et al., RELAP5/MOD2 Models and Correlations, NUREG/CR-5194 (EGG-2531), August 1988.

[31] D. C. Groeneveld, S. C. Cheng and T. Doan, 1986 AECL-UO Critical Heat Flux Lookup Table, Heat Transfer Engineering 7, 1986 (pp. 46-62).

[32] B. S. Shiralkar, et al., The GESTR-LOCA and SAFER Models for the Evaluation of the Loss-of-Coolant Accident, Volume III: SAFER/GESTR Application Methodology, NEDE-23785-1-PA, Rev. 1, October 1984.

[33] P. Saha, A Study of Heat Transfer to Superheated Steam in a 4x4 Rod Bundle, NEDE-13462, June 1976

[34] B. S. Shiralkar, et al., *SBWR Test and Analysis Program Description*, NEDC-32391P, Rev.C, August 1995.

[35] Takashi Hara, et al., *TRACG Application to Licensing Analysis*, (ICONE-7311), 7th International Conference on Nuclear Engineering, Tokyo, April 19-23, 1999.

[36] R. D. Blevins, Applied Fluid Dynamics Handbook, Van Nostrand, 1984.

[37] G. B. Wallis, One-Dimensional Two-Phase Flow, McGraw-Hill, 1969.

ENCLOSURE 3

MFN 06-011

Affidavit

General Electric Company

AFFIDAVIT

I, George B. Stramback, state as follows:

(1) I am Manager, Regulatory Services, General Electric Company ("GE") and have been delegated the function of reviewing the information described in paragraph (2) which is sought to be withheld, and have been authorized to apply for its withholding.

(2) The information sought to be withheld is contained in the GE proprietary report, NEDE-33083P, Supplement 2, *TRACG Application for ESBWR Anticipated Transient Without Scram Analyses*, January 2006. GE proprietary information is identified by a dark red font with double underlines inside double square brackets. Figures and large equation objects are identified with double square brackets before and after the object. In each case, the superscript notation [3] refers to Paragraph (3) of this affidavit, which provides the basis for the proprietary determination.

(3) In making this application for withholding of proprietary information of which it is the owner, GE relies upon the exemption from disclosure set forth in the Freedom of Information Act ("FOIA"), 5 USC Sec. 552(b)(4), and the Trade Secrets Act, 18 USC Sec. 1905, and NRC regulations 10 CFR 9.17(a)(4), and 2.790(a)(4) for "trade secrets" (Exemption 4). The material for which exemption from disclosure is here sought also qualify under the narrower definition of "trade secret", within the meanings assigned to those terms for purposes of FOIA Exemption 4 in, respectively, <u>Critical Mass Energy Project v. Nuclear Regulatory Commission,</u> 975F2d871 (DC Cir. 1992), and <u>Public Citizen Health Research Group v. FDA,</u> 704F2d1280 (DC Cir. 1983).

(4) Some examples of categories of information which fit into the definition of proprietary information are:

    a.   Information that discloses a process, method, or apparatus, including supporting data and analyses, where prevention of its use by General Electric's competitors without license from General Electric constitutes a competitive economic advantage over other companies;

    b.   Information which, if used by a competitor, would reduce his expenditure of resources or improve his competitive position in the design, manufacture, shipment, installation, assurance of quality, or licensing of a similar product;

    c.   Information which reveals aspects of past, present, or future General Electric customer-funded development plans and programs, resulting in potential products to General Electric;

d. Information which discloses patentable subject matter for which it may be desirable to obtain patent protection.

The information sought to be withheld is considered to be proprietary for the reasons set forth in paragraphs (4)a., and (4)b, above.

(5) To address 10 CFR 2.390 (b) (4), the information sought to be withheld is being submitted to NRC in confidence. The information is of a sort customarily held in confidence by GE, and is in fact so held. The information sought to be withheld has, to the best of my knowledge and belief, consistently been held in confidence by GE, no public disclosure has been made, and it is not available in public sources. All disclosures to third parties including any required transmittals to NRC, have been made, or must be made, pursuant to regulatory provisions or proprietary agreements which provide for maintenance of the information in confidence. Its initial designation as proprietary information, and the subsequent steps taken to prevent its unauthorized disclosure, are as set forth in paragraphs (6) and (7) following.

(6) Initial approval of proprietary treatment of a document is made by the manager of the originating component, the person most likely to be acquainted with the value and sensitivity of the information in relation to industry knowledge. Access to such documents within GE is limited on a "need to know" basis.

(7) The procedure for approval of external release of such a document typically requires review by the staff manager, project manager, principal scientist or other equivalent authority, by the manager of the cognizant marketing function (or his delegate), and by the Legal Operation, for technical content, competitive effect, and determination of the accuracy of the proprietary designation. Disclosures outside GE are limited to regulatory bodies, customers, and potential customers, and their agents, suppliers, and licensees, and others with a legitimate need for the information, and then only in accordance with appropriate regulatory provisions or proprietary agreements.

(8) The information identified in paragraph (2), above, is classified as proprietary because it contains the results of TRACG analytical models, methods and processes, including computer codes, which GE has developed, and applied to perform ATWS evaluations for the ESBWR. GE has developed this TRACG code for over fifteen years, at a total cost in excess of three million dollars. The reporting, evaluation and interpretations of the results, as they relate to ATWS evaluations for the BWR was achieved at a significant cost, in excess of one quarter million dollars, to GE.

The development of the evaluation process along with the interpretation and application of the analytical results is derived from the extensive experience database that constitutes a major GE asset.

(9) Public disclosure of the information sought to be withheld is likely to cause substantial harm to GE's competitive position and foreclose or reduce the availability of profit-making opportunities. The information is part of GE's

comprehensive BWR safety and technology base, and its commercial value extends beyond the original development cost. The value of the technology base goes beyond the extensive physical database and analytical methodology and includes development of the expertise to determine and apply the appropriate evaluation process. In addition, the technology base includes the value derived from providing analyses done with NRC-approved methods.

The research, development, engineering, analytical and NRC review costs comprise a substantial investment of time and money by GE.
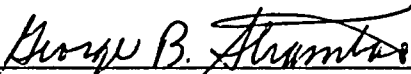
The precise value of the expertise to devise an evaluation process and apply the correct analytical methodology is difficult to quantify, but it clearly is substantial.

GE's competitive advantage will be lost if its competitors are able to use the results of the GE experience to normalize or verify their own process or if they are able to claim an equivalent understanding by demonstrating that they can arrive at the same or similar conclusions.

The value of this information to GE would be lost if the information were disclosed to the public. Making such information available to competitors without their having been required to undertake a similar expenditure of resources would unfairly provide competitors with a windfall, and deprive GE of the opportunity to exercise its competitive advantage to seek an adequate return on its large investment in developing these very valuable analytical tools.

I declare under penalty of perjury that the foregoing affidavit and the matters stated therein are true and correct to the best of my knowledge, information, and belief.

Executed on this 12th day of January 2006

George B. Stramback
General Electric Company